Performance of Ultra Shallow Floor Beams (USFB) exposed to standard and natural fires

Naveed Alam[1], Chrysanthos Maraveas[2], Konstantinos Daniel Tsavdaridis[3], Ali Nadjai[1]

[1]FireSERT, School of Built Environment, Ulster University, Belfast, UK
[2]Department of Civil Engineering, University of Patras, Patra, Greece
[3]School of Civil Engineering, University of Leeds, Leeds, UK

Corresponding author: C. Maraveas: c.maraveas@maraveas.gr

Abstract

This paper investigates computationally the fire performance of a plug steel-concrete composite flooring system, the partially encased ultra-shallow floor beams (USFB). The investigation of the behaviour of USFBs exposed to standard and natural fires is crucial in determining their fire resistance and evaluating their overall performance in contemporary construction. Although the product providers usually indicate the fire resistance of USFBs based on EN1994-1-2 procedures, the response to elevated temperature effects remains yet neither well documented nor clearly understood. This analysis involves two different beams of 5m and 8m span. Results show that the unprotected beams experience severe temperature gradients while exposed to standard fire, as the lower flange still remains unprotected in contrast to the upper steel parts of the cross-section which are encased in concrete. Their fire resistance rating is found approximately at 40 mins. Moreover, different thermal gradients are developed when the USFBs are exposed to natural fires (slow and fast burning). When the lower flange is protected with intumescent coatings, the USFBs have shown increased fire resistance and they can survive a full duration of a natural fire under realistic utilization ratios. From the parametric analyses, the optimized thicknesses for the required intumescent coating were obtained to achieve 60, 90, and 120 min of fire resistance and for surviving of natural fires exposures.

Keywords: Ultra Shallow Floor Beams; Flooring systems; Fire resistance; Intumescent coating; Fire; Standard Fire; Natural Fires

Introduction

The design of composite steel-concrete beams has evolved over the years and significant improvements have been seen in the last three decades. One of these innovative designs is the Ultra-shallow floor beam (USFB) with plug composite system. These beams were developed and introduced in UK in 2006 by Westok Ltd. (UK). USFBs are formed by welding two highly asymmetric steel Tees, cut from a universal beam section and a universal column section, along their web. The lower Tee is usually larger as compared to the upper Tee. USFBs can be used with pre-cast concrete slabs as well as with deep steel decking; the latter offers a decreased self-weight and thus is more popular [1]. The steel web of these beams has continuous periodical web openings along the length, alike cellular beams, as a result concrete passes through these openings during casting and provides connectivity to the concrete slab on both sides. This concrete between the flanges and in the openings can enhance the longitudinal and vertical shear strength of the USFBs [2].

When comparing USFBs with normal composite steel-concrete beams (down-stand beams), USFBs are far shallower systems thus reducing the structural depth significantly. The shear connection is very strong in comparison to standard headed shear studs on the top of the steel flange in down-stand beams, due to the concrete which is passing through some web openings and it provides continuity to the slab, with the use of either tie-bars, horizontally web-welded shear studs, or ducting. Full service integration can be achieved when deep profiled steel decking is employed, as pipes or ducks pass through the beam, between the ribs of the steel decking, and typically every few web openings which are not filled by concrete. In the case of precast units, all web openings are filled by in-situ concrete to provide the cohesion between the precast units and the steel beam, hence service integration is not provided. This concrete plug system forms a unique mechanism for transferring longitudinal shear forces along the beam. Moreover, the asymmetric perforated steel beam does not buckle as the beam is partially encased by the concrete, which also provides added fire resistance to the steel as opposed to down-stand beams. Furthermore, USFBs minimise the need for propping during construction.

Extensive research has been conducted to study the response of USFBs at ambient temperatures via experimental investigations and finite element modelling (FEM). These studies include investigations on their horizontal shear resistance [3], their vertical shear resistance [4] as well as their vibration performance [5] at ambient temperatures. Although experimental and analytical investigations are available related to the performance of USFBs at ambient temperatures [2,4], the studies addressing their performance at elevated temperatures are limited to a study related to the unprotected USFBs exposed to standard fire [6]. Despite the unavailability of satisfactory studies related to their fire performance, the manufacturing companies certify their fire resistance and insulation requirements based on the Eurocode procedures, EN 1994-1-2 (2014)[7].

Having recognised the existing knowledge gaps with regards to the applicability of the Eurocodes related to their fire performance, a detailed investigation was conducted herein to understand the performance of unprotected as well as protected USFBs exposed to standard and natural fires. Previous studies have shown that natural fires result in different temperature distributions and thermal gradients and significantly affect the performance of partially protected steel beams [8,9]. FEM was conducted using the commercial programme ABAQUS version 2019. The methodology used in this research follows the same principles and procedures used to successfully simulate the performance of asymmetric slim floors in fire against fire test results as presented by Alam et al, 2018 [8] and Maraveas et al, 2012 [10].

To study the performance of protected and unprotected USFBs, FEM was performed for two simply supported specimens; a 5 m span and a 8 m span. Further details related to sizes, shapes and arrangements are available in Maraveas et al, 2015 [6]. A summary of these details is reproduced in section 2 for the ease of the reader.

The basic findings of the research are that USFBs can survive of a parametric fire with minimum of protection. On the contrary, to archive high fire resistance when exposed to standard fires, USFBs require thick layer of intumescent coating or a combination of low load ratio and protection with intumescent coating.

1. USFB SYSTEM DETAILS

As Ultra-Shallow Floor Beams (USFB) connect with the floor slab on both sides of the steel web via the concrete passing through the web opening [4] (Figure 1). Such slim-floor type composite systems also have other advantages, including increased load carrying capacity, fire resistance, local buckling stiffness and a significant increase in the bending stiffness due to the plug mechanism when compared with traditional steel-concrete composite beams. The plug composite actions is achieved through various ways most commonly by providing steel reinforcement through the web openings perpendicular to the steel beam section as shown in Figure 1 (c). In other words, the reinforcement is transverse to the web of the beam and is passing via the web openings to develop the continuity from one side to the other, and thus increase the longitudinal shear (See Figure 1c). This is called a plug system. In addition, these structures reduce construction cost by eliminating the construction time and reducing the requirements of formwork – no need for slab propping [2,11].The most common applications of USFBs have been with slabs having depths ranging from 180mm to 300mm, in which the concrete has been placed level with the top flange. The practical span to depth ratio of USFBs is usually in the range of 25 to 30. Consequently, the USFB is limited to a span up to 9m, with a depth of up to 300mm. When the span is extended to more than 9m, the depth will increase to more than 300mm, even when lightweight concrete is used [2,11]. This results to an uneconomical solution for flooring systems. Moreover, an increase of slab spans reduces the natural frequencies of the USFBs, leading to an increase of the floor vibration [5].

(a)

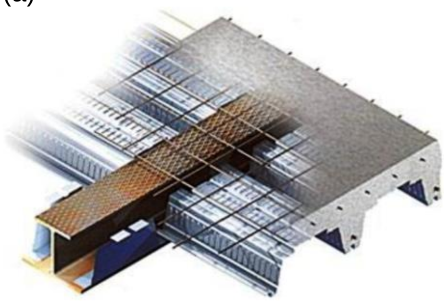

(b)

(c)

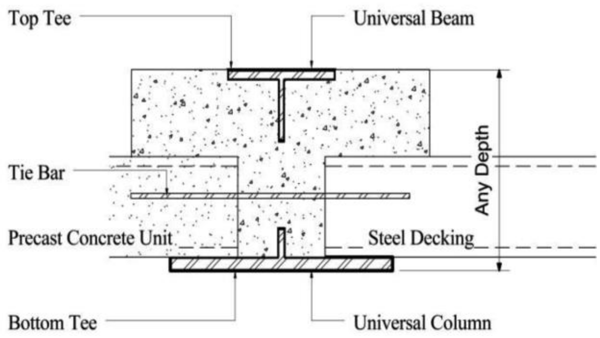

Figure 1. (a), (b) construction arrangements of USFBs [1] and (c) typical cross-section of USFBs [5]

2. SIMULATED USFB SYSTEMS

During this investigation, two typical USFBs have been analysed. Both beams are considered as simply supported. USFB-1 has a 5 m span and has a total section depth of 220 mm. The top Tee of the USFB section is cut from a 254 x 146 x 37 UB section while the bottom Tee has been taken from 254 x 254 x 167 UC section as shown in Figure 2(a). USFB-2 had an 8 m span and consisted of a 254 x 254 x 167 UC top Tee and a 356 x 406 x 235 UC bottom Tee (Figure 2b). Additionally, two steel reinforcing bars were applied to the tension zone of USFB-2 to replicate the construction practices. In both cases, the effective width of the USFB assemblies has been taken equal to L/8 for analytical modelling purposes. The maximum load capacities for these specimens were calculated and presented earlier by Maraveas et al (2015)[6] which have been adopted during this study.

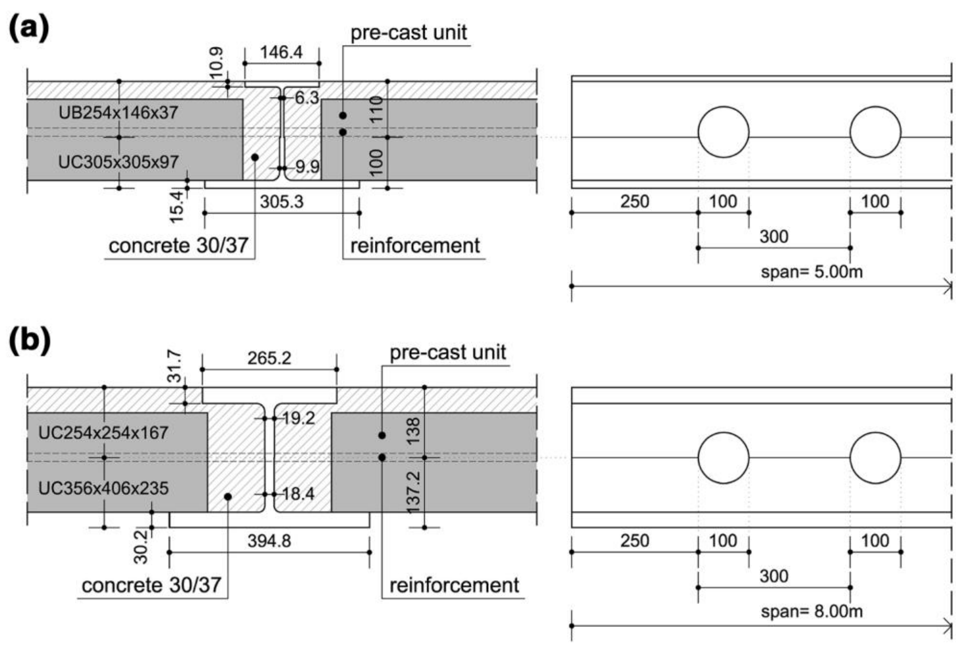

Figure 2. Details of the USFBs used for numerical simulation (a) Beam A and (b) Beam B [6].

3 Numerical Modelling

3.1 Material Properties

The material properties for structural steel, steel reinforcement and the concrete are adopted following the recommendations of the Eurocodes, EN 1994-1-2 (2014) [7]. The material stress-strain relationships at room temperature are based on the design values defined in Eurocodes. The material safety factor considered according to UK National Annex for fire design (γ_M=1,00) for structural steel, steel reinforcement and concrete. The structural steel was modelled using a yield strength of 355 MPa while the concrete was modelled with a compression strength of 35 MPa. Further, the tensile strength of the concrete was also considered following the recommendations of the Eurocodes, EN 1994-1-2 (2014) [7]. The density of concrete was taken 2400 kg/m^3 for concrete while the same was taken 7850 kg/m^3 for the structural and reinforcing steel. The thermal properties (thermal conductivity and specific heat), the mechanical properties and thermal expansion of steel and concrete are taken from EN 1994-1-2 (2014) [7].

3.2 Modelling of intumescent coatings

The fire protection material used during this investigation is in the form of intumescent coatings. The behaviour of intumescent coatings in fire has been of great interest amongst the researchers in the recent past and numerous publications are available. The majority of the literature focuses on their behaviour under cone calorimeters or in standard fire exposure conditions similar to the work conducted by de Silva et al (2019) [12]. The section factors used during these investigations are also limited. A detailed literature review on the performance of intumescent coatings exposed to different scenarios suggests that one of the most comprehensive experimental studies in this regard was conducted by Cirpici et al (2016) [13]. In additional to the standard fire, two natural fire scenarios, a fast fire and a slow fire, were also considered during the investigation. During the research conducted by Cirpici et al (2016) [13], various investigations were carried out to analyse the behaviour of intumescent coatings applied to steel specimens with different section factors. These section factors were 333 m^{-1}, 200 m^{-1}, 100 m^{-1} and 50 m^{-1}. In addition, the effectiveness of the thicknesses of intumescent coatings was investigated considering specimens with thickness of intumescent coatings equal to either 0.4 mm, 0.8 mm, 1.2 mm, 1.6 mm, or 2.0 mm.

During this study, the specific heat of the intumescent coatings is taken as 1000 J/kg K and the density is 1300 kg/m^3 as proposed by Dai et al (2010) [14]. It is considered that the quantity of intumescent coatings is significantly smaller as compared to the structural elements, i.e., the influence of density and specific heat is insignificant considering the heat transfer through intumescent coatings being predominantly via conduction [12]. The thermal conductivity of intumescent coating is taken considering its dependency on fire exposure conditions (heating rate), the section factors as well as its thickness. During this investigation, three fire exposure scenarios are considered, the standard fire, the fast-natural fire, and the slow natural fire. Three different thicknesses of the intumescent coatings are considered, 1.2 mm, 0.8 mm and 0.4 mm. It was found that the section factors for USFB-1 (Figure 2(a)) and USFB-2 (Figure 2(b)) were 73 m^{-1} and 37 m^{-1}, respectively. To obtain the temperature dependent thermal conductivity for these section factors, linear interpolation and extrapolation was conducted using the values reported for section factors 100 m^{-1} and 50 m^{-1} by Cirpici et al (2016)[13]. The values of temperature dependent thermal conductivity of intumescent coating for section factors 73 m^{-1} and 37 m^{-1} under different fire exposure conditions are presented in Figure 3 for thickness 1.2 mm, 0.8 mm, and 0.4 mm, respectively. These values have been used for the analytical modelling of thermal performance of intumescent coatings during this investigation.

The contribution of intumescent coatings towards the mechanical response of the protected USFBs is considered negligible. Hence, no mechanical properties have been used during the analytical modelling.

(a)

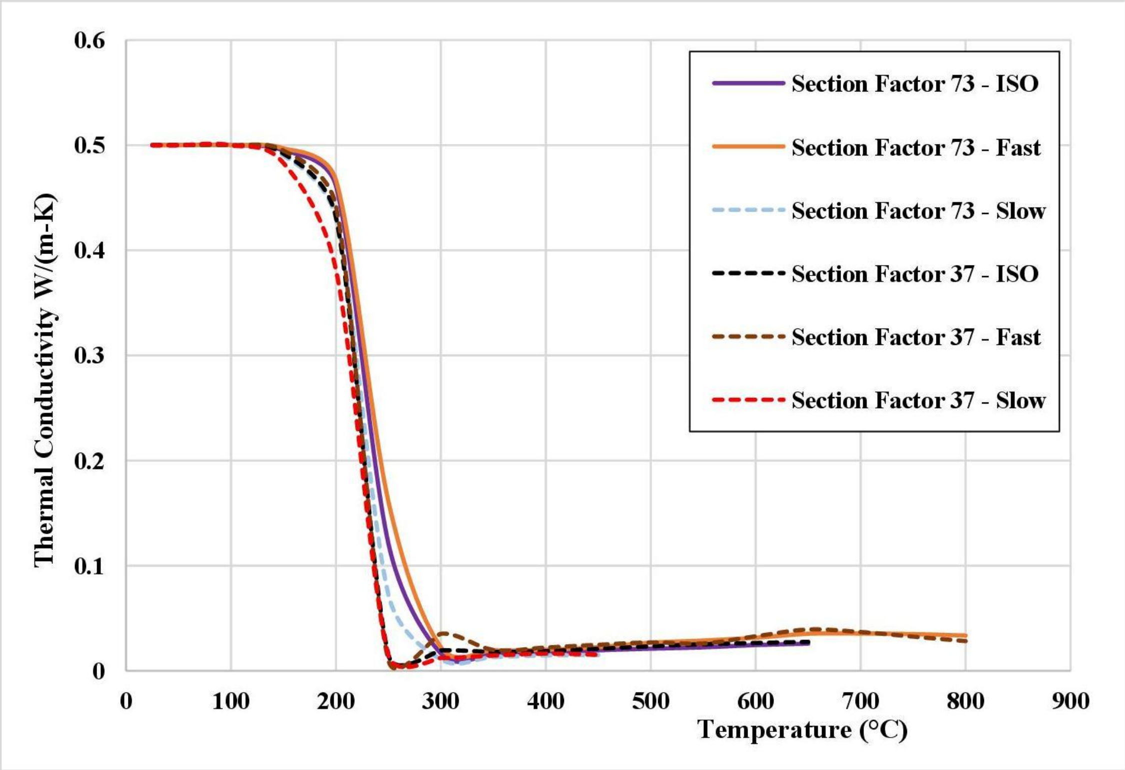
0.6
0.5
0.4
0.3
0.2
0.1
0
Thermal Conductivity W/(m-K)
0
100
200
300
400
500
600
700
800
900
Temperature (°C)
Section Factor 73 - ISO
Section Factor 73 - Fast
Section Factor 73 - Slow
Section Factor 37 - ISO
Section Factor 37 - Fast
Section Factor 37 - Slow

(b)

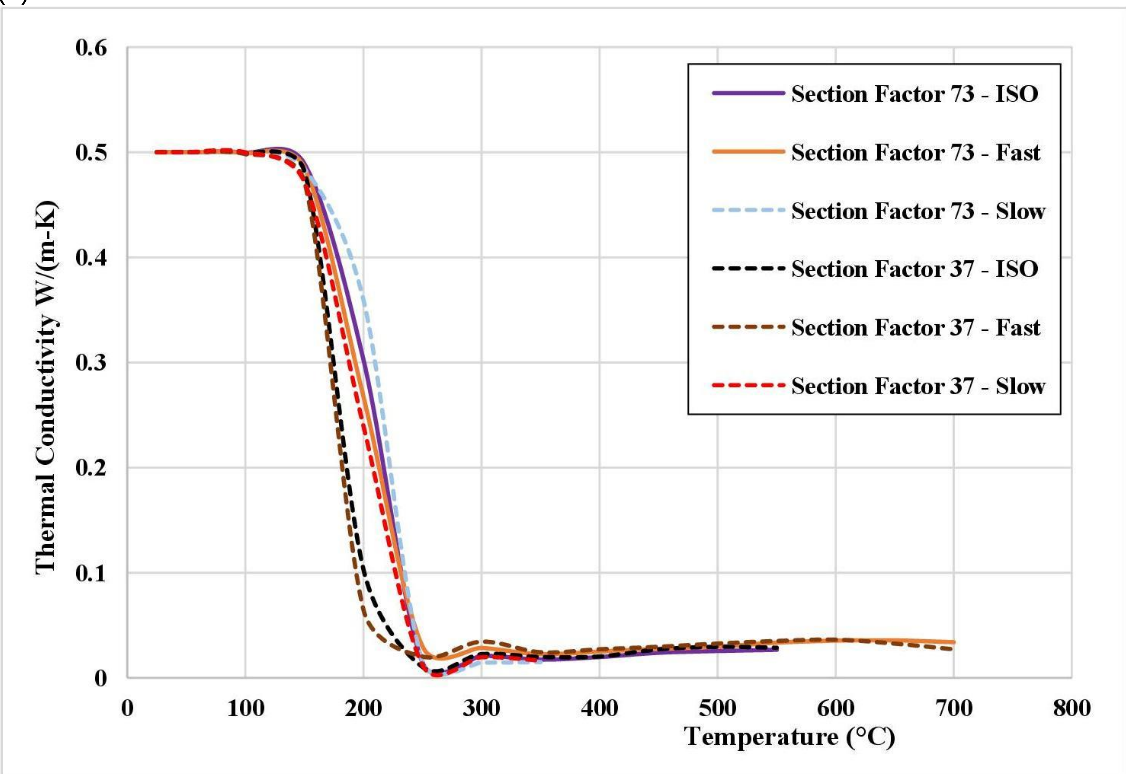
0.6
0.5
0.4
0.3
0.2
0.1
0
Thermal Conductivity W/(m-K)
0
100
200
300
400
500
600
700
800
Temperature (°C)
Section Factor 73 - ISO
Section Factor 73 - Fast
Section Factor 73 - Slow
Section Factor 37 - ISO
Section Factor 37 - Fast
Section Factor 37 - Slow

(c)

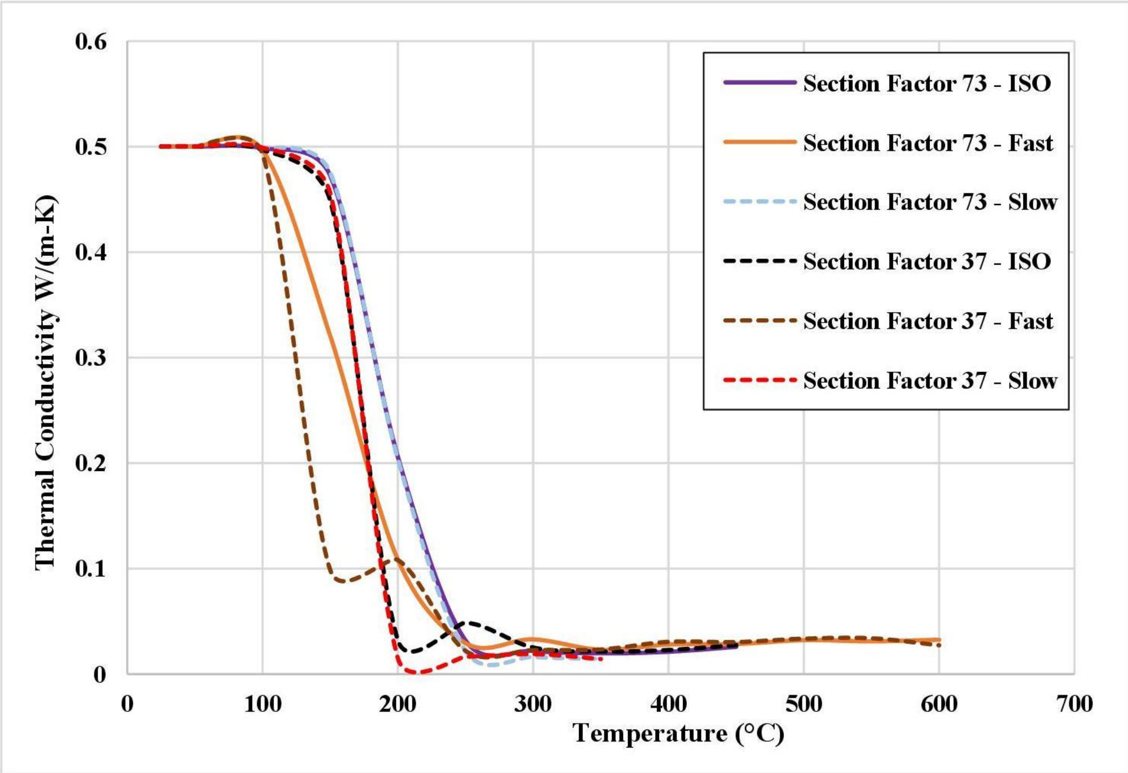

Figure 3. Temperature dependent thermal conductivity for intumescent coating with (a) 1.2 mm thickness under different fire exposure conditions for section factors $73m^{-1}$ and $37m^{-1}$, (b) 0.8 mm thickness under different fire exposure conditions for section factors $73m^{-1}$ and $37m^{-1}$ and (c) 0.4 mm thickness under different fire exposure conditions for section factors $73m^{-1}$ and $37m^{-1}$

3.3 The fire exposure conditions

Eurocodes provide different fire exposure scenarios in terms of standard fire models as well as the natural fire models in section 3.2 and 3.3 of EN 1991-1-2 (2009)[15]. The fire exposure scenarios used during this research are presented in Figure 4.

The natural fire curves shown in Figure 4 have been produced according EN 1991-1-2 (2009) [15]. For this purpose, the fire compartment has been assumed to be a representative of an office building with a fire load density ($q_{t,d}$) equal to 200 MJ/m^2. The representation of compartment boundaries in terms of density, specific heat and thermal conductivity are taken in terms of 'b' as defined in EN 1991-1-2 (2009)[15]. The value of 'b' is equal to 1120 $J/M^2s^{1/2}K$ both for the fast and the slow natural fire. The value of opening factor for the fast fire is taken equal to 0.1 $m^{1/2}$ while the one for the slow fire is taken as 0.02 $m^{1/2}$ - the minimum value proposed by EN 1991-1-2. These parametric fires cover a wide range of natural (compartment) fires enabling its general applicability. A similar approach is previously used by Alam et al (2018) [16] to study the response of slim floors beams at elevated temperatures.

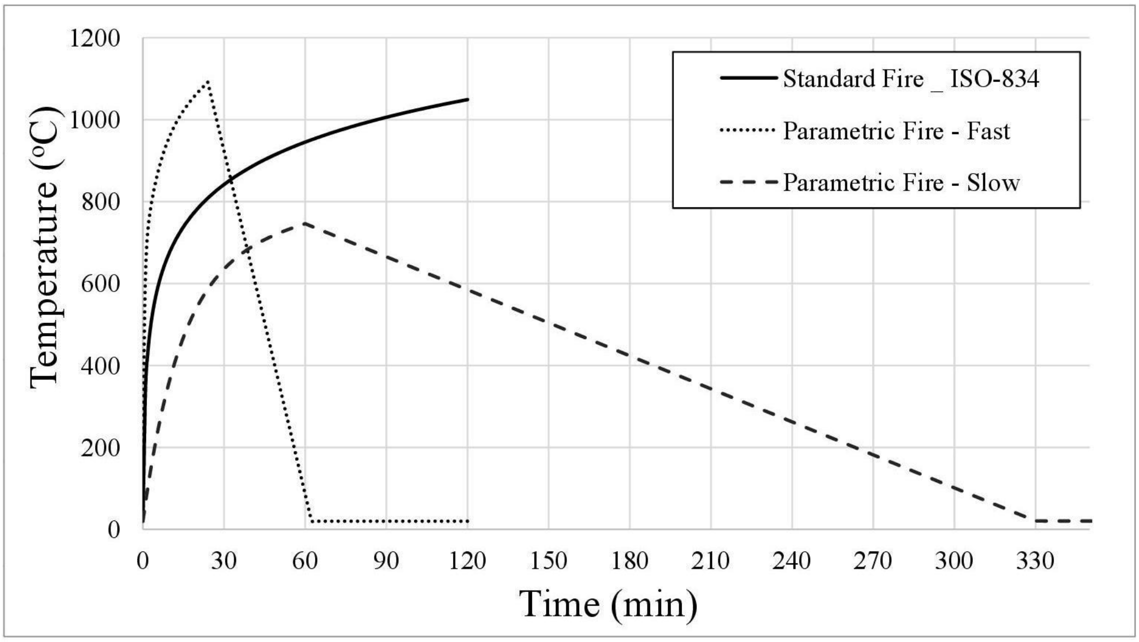

Figure 4. Considered standard and natural fire curves

3.4 Numerical Modelling

3.4.1 Unprotected USFBs

Finite element modelling for the unprotected USFBs is performed using the two-phase method explained and presented by Maraveas et al (2015) [6]. In the initial phase, temperature contours for the USFBs are obtained by performing the thermal analysis. The convection coefficients for exposed and unexposed surfaces are taken equal to 25 W/m^{2}K and 9 W/m^{2}K, respectively. The radiation emissivity for the bottom steel flange and the composite floor is taken as 0.7 following the EN1994-1-2 (2014) [7] recommendations. Both concrete and steel are modelled using the 8-node linear brick elements, DC3D8 and the interface between the steel and the concrete is modelled as a perfect thermal contact allowing full heat transfer. For each unprotected USFB, three thermal analyses are performed - the standard fire exposure conditions, the fast natural fire and the slow natural fire. Details related to the fire exposure conditions are provided earlier in section 3.3.

The second phase of the numerical modelling consists of the thermo-mechanical analysis and is performed in two steps. During the first step, external loads representing the degree of utilization of USFBs are applied while in the second step, the USFB specimens are heated using the thermal contours obtained during the first phase. The external loads applied were uniformly distributed along the length of each beam. The concrete part is modelled using 8-node linear brick elements (C3D8) considering the numerical instabilities associated with the inelastic behaviour of concrete. On the other hand, the steel parts of the USFBs are modelled using hexahedral elements with reduced integration (C3D8R). The analytical modelling was conducted for USFBs under 55%, 70%, and 100% degrees of utilizations.

3.4.2 Protected USFBs

The protected USFB specimens were similar to the unprotected specimens with the exception of a layer for intumescent coating modelled over the exposed bottom flange of the steel section. The boundary conditions of the thermal analysis and the position of the insulation are shown in Figure 5. Three FE models were prepared for each USFB. The first model consisted of an intumescent layer of 1.2 mm on the exposed bottom flange while the second consisted of a 0.8 mm layer of protection. The last USFB model consisted of a 0.4 mm thick layer of intumescent coating. The thermal analysis was performed using the 8-node linear brick elements, DC3D8 for concrete, steel, and the intumescent coating. The convection coefficient and radiation emissivity for exposed and unexposed surfaces of concrete and steel were same as that used for the unprotected USFBs. However, the convection coefficient and radiation emissivity for the intumescent coatings was taken as 20 W/m^2K and 0.95, respectively as proposed by Bourbigot et al (1995) [17]. A similar approach is also used by Alam et al (2018) [8] to study the performance of protected slim floor beams exposed to elevated temperatures. The thermal analysis for protected USFBs was performed for the three fire exposure scenarios discussed in section 3.3.

During the thermo-mechanical analysis, no contribution of the intumescent coating was considered as this material was only meant to protect against the elevated temperatures. The thermo-mechanical analysis was the two-step method detailed earlier in section 3.4.1. Similar to the unprotected case, the performance of USFBs was investigated for three degrees of utilizations, 55%, 70%, and 100%.

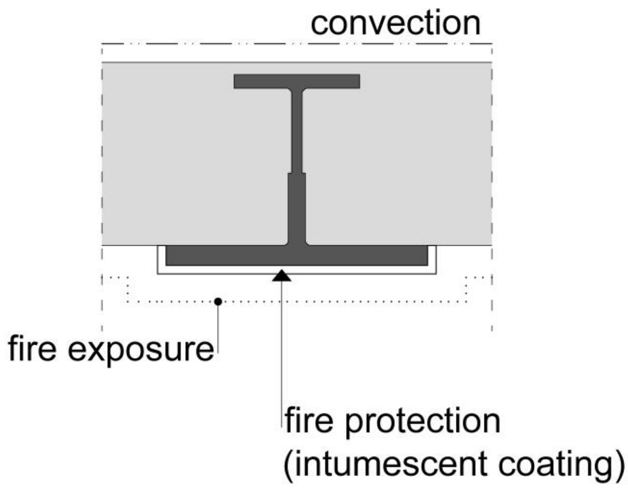

Figure 5. Thermal analysis boundary conditions and the protected surface of the steel cross-section with intumescent coating.

3.5 Validation of numerical models

Fire tests on USFBs do no exist. For this reason, the validation performed against fire tests from similar flooring systems. The methodology used during this research follows the same principles and procedures used to successfully simulate the performance of asymmetric slim floors in fire [10, 16] against fire test results. More specifically, two slim floor fire tests performed at Warrington Fire Research Centre were successfully simulated with use of the described methodology in previous sections in [10, 16]. Furthermore, validation of the used numerical methodology for protected slim floors presented in section 3.2 is presented in [16].

3.6 Load factor

According EN1994-1-2 (2009) [7], the design loads for the fire situation are given by the equation:

$$E_{fi,d} = n_{fi} E_d \tag{1}$$

where E_d is the design value of the corresponding force for a fundamental combination of actions, $E_{fi,d}$ is the design forces for fire design and n_{fi} is the reduction factor of E_d or called for simplicity as load factor.

The load factor n_{fi} is a function of the reduction factor ψ_{fi} ($\psi_{1,1}$ or $\psi_{2,1}$) and of the ratio $Q_{k,1}/G_k$ and practically can take values between 0.75 and 0.25. EN1994-1-2 (2009) (Figure 6) suggests values of n_{fi} 0.65 or 0.70 (depending the use of the structure) for simplicity and without detailed calculation. This is a conservative assumption. Bailey (1999) [18] states that the loads expected in a fire event are in the range of 50 to 55% of the capacity of the structural members at ambient temperatures.

As the load factor cannot be determined, this research has a more general purpose, the analysis is performed for load factors 55%, 70%, and 100%. It must be noted that the load factor 100% is not realistic and only included for comparison purposes. The ambient temperature loads are described in Maraveas et al (2015) [6]. The load applied as uniform load, before heating.

As the load factor is relevant to the applied design loads (E_d), the capacity of the structural element should be higher than E_d. In order to estimate the over-strength which may appear, information regarding the design per EN1994-1-1 (2004) [7] are presented in Table 1.

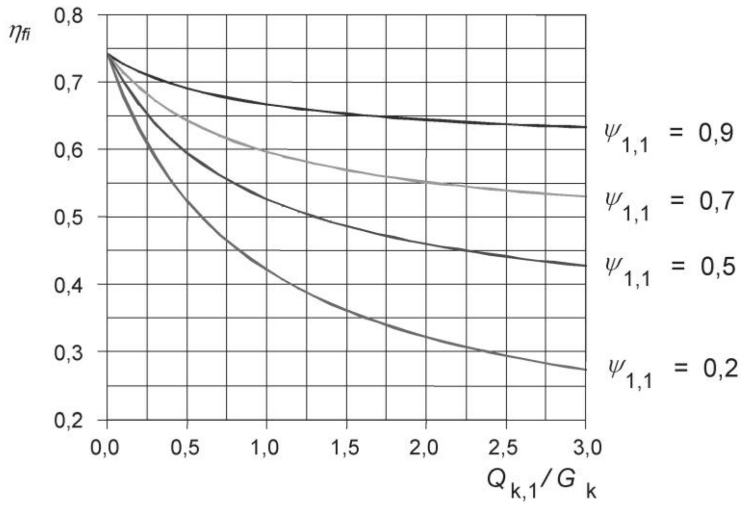

Figure 6. Reduction factor of the design value of the corresponding force for a fundamental combination of actions n_{fi} as a function of the ratio $Q_{k,1}/G_k$ and $\psi_{1,1}$ [7].

Table 1 Normal temperature maximum design unity factors for the critical load combination [6]

Failure mode	**Beam A**	**Beam B**
Vertical shear	0.51	0.41

Horizontal shear	0.98	0.76
Moment shear interaction	**1.00**	0.91
Vierendeel bending	**1.00**	0.91
Longitudinal shear in slab	0.16	0.14
Vibration (Hz)	5.49	**3.27**
Imposed deflection (mm)	8.18	19.03

4. FEM Results

4.1 Evaluation of numerical results

The performance of USFB assemblies has been analysed following the deflection based failure approach proposed in the British and International Standards. According to the British Standards, BS 476 Part-20 (1999) [19] and ISO 834–1 (1987) [20], failure is deemed to occur once the mid-span deflection of beams exceeds L/20 or the rate of deflection exceeds $L^2/9000d$, L is the span while d is the overall depth of beam. The rate of deflection criteria is only applicable once the mid-span deflection exceeds L/30 limits.

4.2 Performance of unprotected USFBs

In this section, the performance of unprotected USFBs is discussed in terms of developed temperatures (thermal response) and fire resistance (structural response).

4.2.1 Thermal response

The temperature – time relationships for different fire exposures at different characteristic nodes are presented in Figure 7. For both beams, the developed temperatures in nodes 3, 4, and 7 are very low and, practically, the temperature does affect the mechanical properties of steel (<400 ^{o}C). As the shear connection between the steel beam and the concrete is undertaken due the friction between the steel and concrete and via the concrete resistance and a tie bar in the web opening while the developed temperatures are low, the shear connection is not affected by the fire exposure. Similarly, approximately the 66% of the web develops temperatures lower than 400 ^{o}C, hence, the effect on its shear resistance is minimum.

As only the bottom flange is exposed to fire, it develops high temperatures (nodes 1 and 2, Figure 7). The developed temperatures are higher in node 1 as it is near the corner of the bottom flange – i.e., near the two exposed sides. Node 2 develops lower temperatures in comparison to node 1, as the web absorbs the heat.

From the diagrams in Figure 7, it is clear that extreme thermal gradients are developed across the USFBs. These thermal gradients depend on the fire exposure type. When the beam is heated against the fast fire curve (Figure 4), due to the extremely rapid heating rate, the steel cross-section develops extreme thermal gradients. When the beam is exposed to slow fire, the heating is slow and for a longer duration, so the cross-section develops lower thermal gradients and the developed temperatures are more uniform. When standard fire is used, the thermal gradients are in between those obtained for fast and slow fires. For Beam A, the maximum temperature is developed at node 1 for fast and slow fire exposures, the comparisons of temperature profiles are presented in Tables 2 and 3, respectively. It must be noted that the concrete slab develops higher thermal gradients than the steel section, given that the ratio of the thermal conductivity of steel to the thermal conductivity of concrete is approximately five times. The thermal gradients are increased, e.g., the non-uniform temperature distribution, when the height of the cross-section is increased. Hence, Beam B (Figure 7(d), (e), (f)) with cross-section height of 275.2 mm develops higher thermal gradients in comparison with Beam A (Figure 7(a), (b), (c)) with cross-section height 200 mm.

(a)

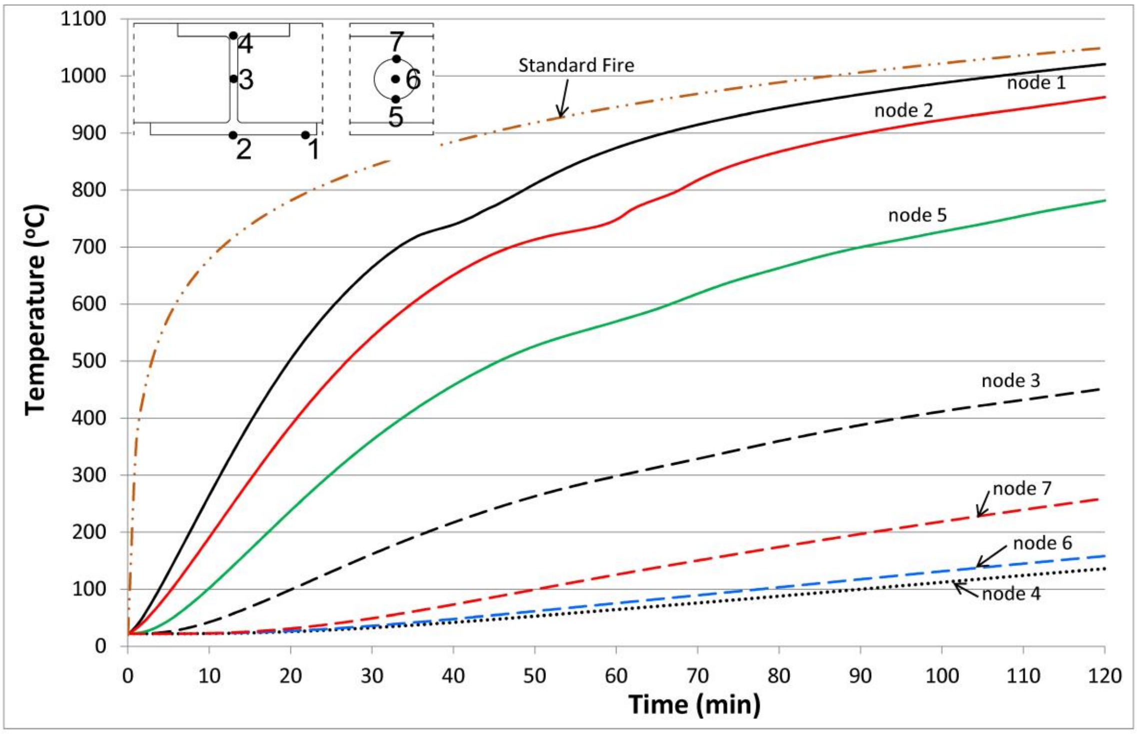
Standard Fire
node 1
node 2
node 5
node 3
node 7
node 6
node 4
Temperature (ºC)
Time (min)
4
3
2
1
7
6
5

(b)

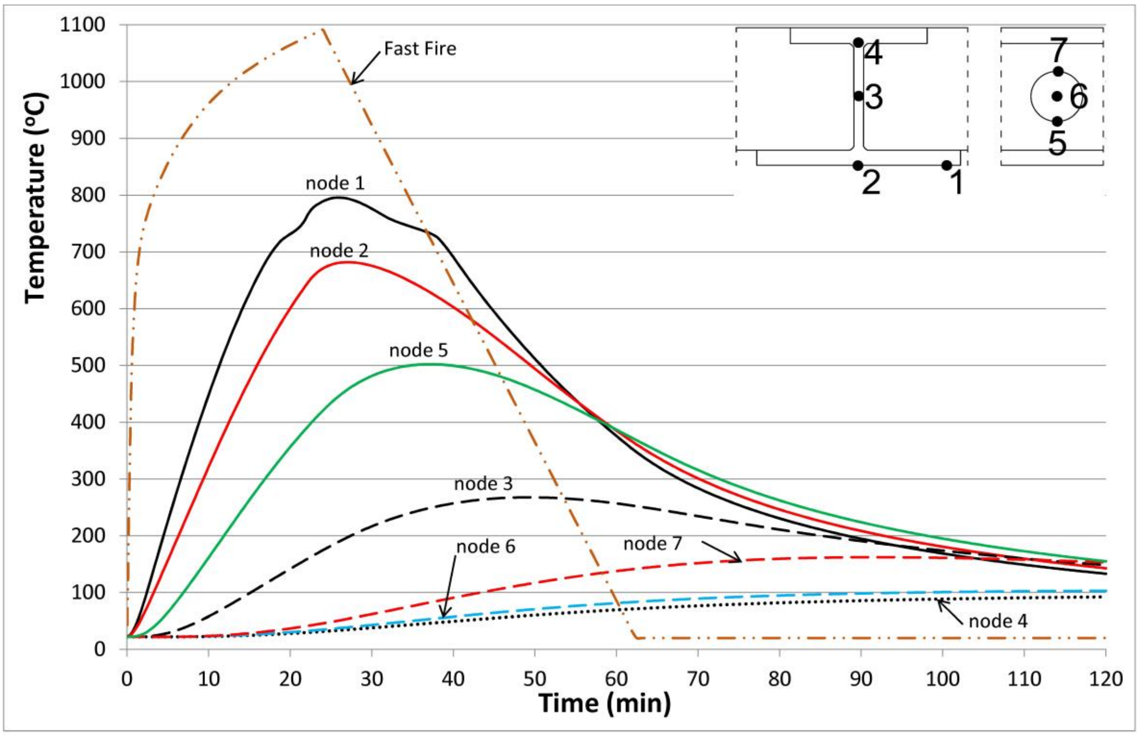
Fast Fire
node 1
node 2
node 5
node 3
node 6
node 7
node 4
Temperature (ºC)
Time (min)
4
3
2
1
7
6
5

(c)

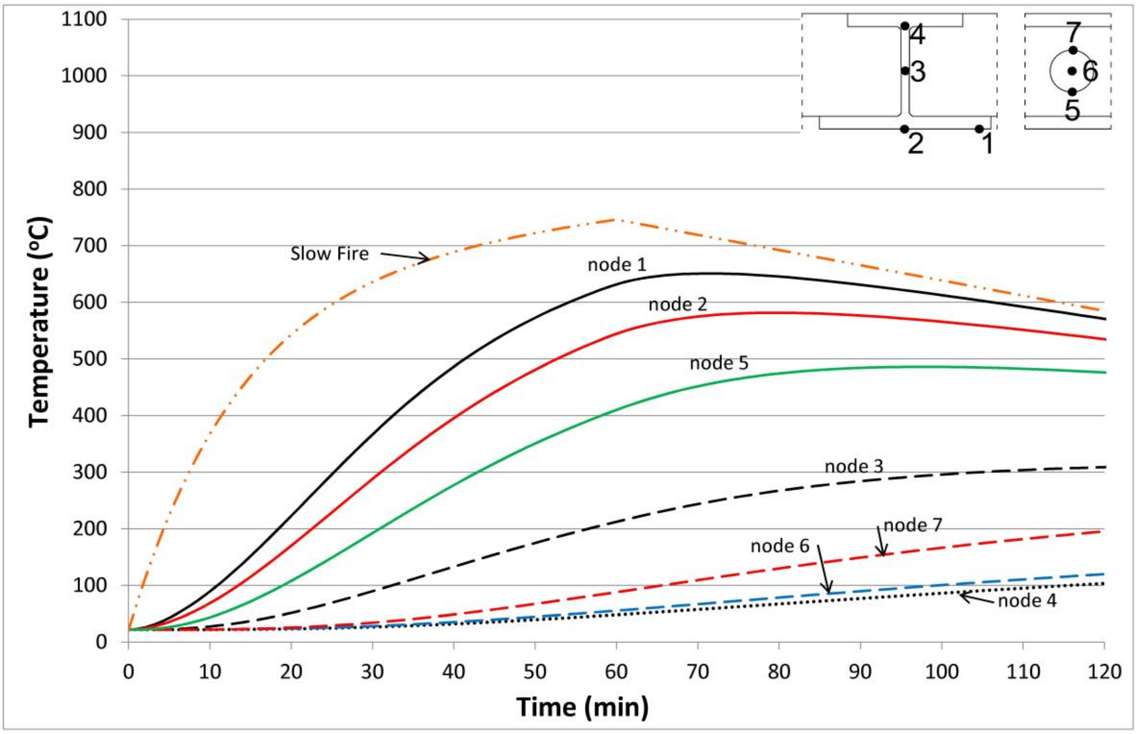
Temperature (ºC)
Time (min)
1100
1000
900
800
700
600
500
400
300
200
100
0
0
10
20
30
40
50
60
70
80
90
100
110
120
Slow Fire
node 1
node 2
node 5
node 3
node 7
node 6
node 4
4
3
2
1
7
6
5

(d)

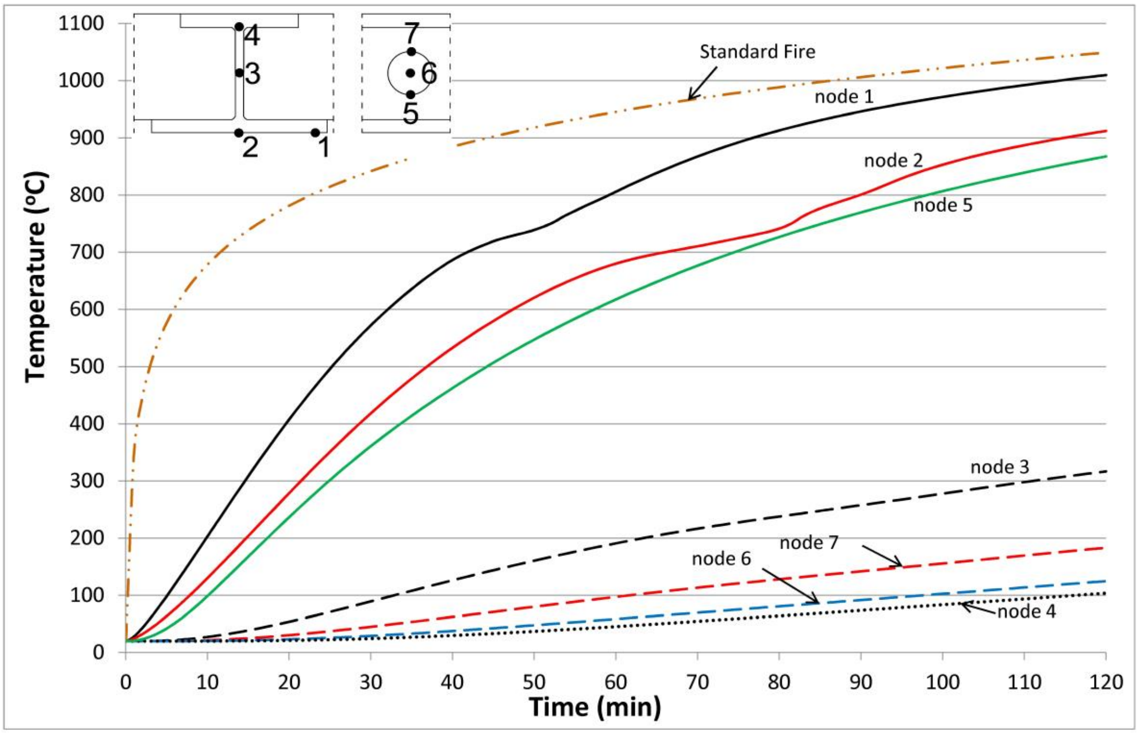
Temperature (ºC)
Time (min)
1100
1000
900
800
700
600
500
400
300
200
100
0
0
10
20
30
40
50
60
70
80
90
100
110
120
Standard Fire
node 1
node 2
node 5
node 3
node 7
node 6
node 4
4
3
2
1
7
6
5

(e)

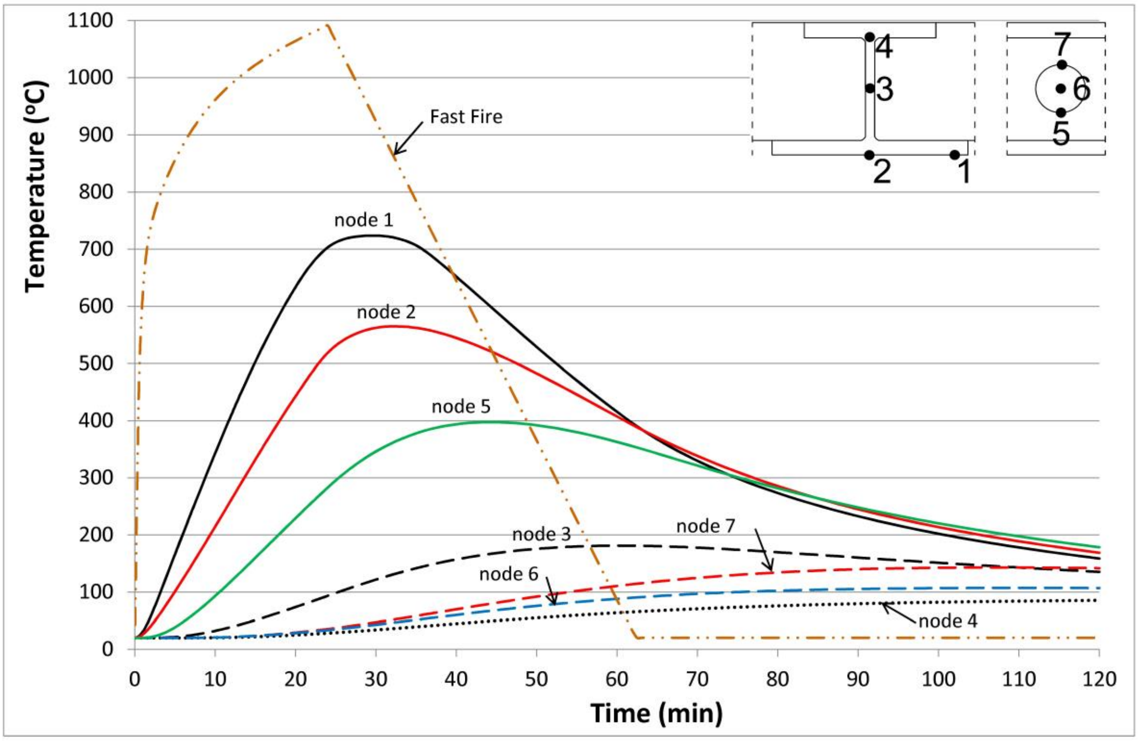

(f)

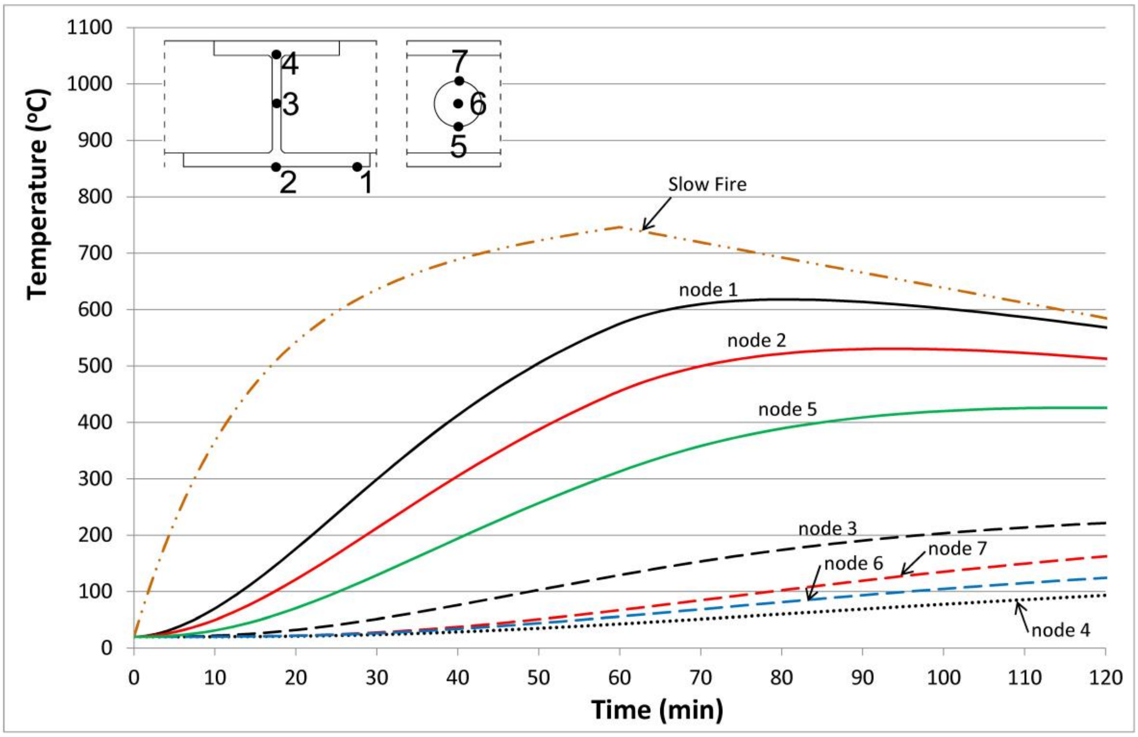

Figure 7. Temperature vs time relationships for unprotected Beam A and (a) standard fire, (b) fast fire, (c) slow fire exposure and for unprotected Beam B and (d) standard fire, (e) fast fire, (f) slow fire exposure.

Table 2 Developed temperatures for different fire exposures for the maximum developed temperature at node 1 with slow fire exposure (θ=650 ^{o}C) for Beam A.

Fire Exposure Node No According Figure 7	Slow Fire t = 73.07 min	Fast fire t = 16 min	Standard fire t = 29.33 min
Node 1	650 ^{o}C	656 ^{o}C	655 ^{o}C
Node 2	578 ^{o}C	502 ^{o}C	533 ^{o}C
Node 5	460 ^{o}C	283 ^{o}C	354 ^{o}C
Node 3	252 ^{o}C	107 ^{o}C	157 ^{o}C

Table 3 Developed temperatures for different fire exposures for the maximum developed temperature at node 1 with fast fire exposure (θ=796 ^{o}C) for Beam A. Results for slow fire exposure are not presented, as node 1 does not reach the target temperature pf 796 ^{o}C.

Fire Exposure Node No According Figure 7	Fast fire t = 25.95 min	Standard fire t = 48.33 min
Node 1	796 ^{o}C	797 ^{o}C
Node 2	680 ^{o}C	706 ^{o}C
Node 5	433 ^{o}C	517 ^{o}C
Node 3	189 ^{o}C	256 ^{o}C

4.2.2 Structural response

The simulation results for the unprotected Beam A are presented in Figure 8(a). The initial slopes of the mid-span deflection are affected by different thermal gradients as discussed in the previous section. When Beam A is exposed to the fast fire, the fire resistance is limited to 15 and 20 min for load factors 100% and 70%, respectively. Under the same fire conditions, Beam

A survives the full duration of the fast fire when the load ratio is 55%. Beam A also survives the full duration of the slow fire for all load factors applied. The fire resistance, when exposed to the standard fire, is between 30 and 50 min depending on the applied load factor.

From the structural analysis of the unprotected Beam B presented in Figure 8(b), similar results to those for Beam A are obtained. When it is exposed to standard fire, the fire resistance is limited between 35 and 45 mins for the various load factors, despite that it has higher section factor and some over-strength in bending. When exposed to the slow parametric fire, Beam B survives the full duration of the slow fire for load factors 55% and 70%. When the load factor is 100% the beam fails after 65 min of slow fire exposure. Similarly, for the fast parametric fire exposure, when the applied load factor is 100% the beam has fire resistance less than 20 min. For lower load factors than 100%, the fire resistance is approximately 20 min. The fire resistance is limited in these cases (fast fire exposure, load factors 70% and 55%) due to the excessive deformation caused by thermal gradients. As it can be seen in Figure 8(b), Beam B survives the full duration of the fast fire for these load factors, and if a performance-based approach was employed, the fire resistance could be estimated as R120 or higher.

(a)

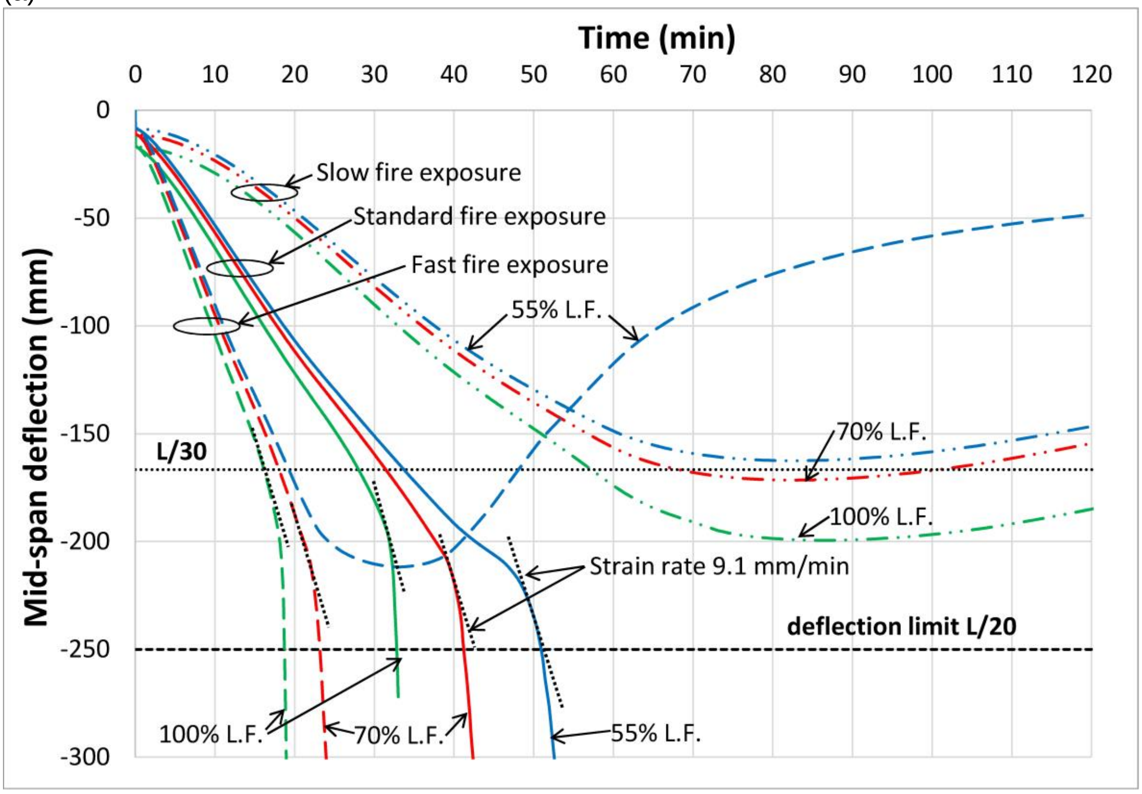

(b)

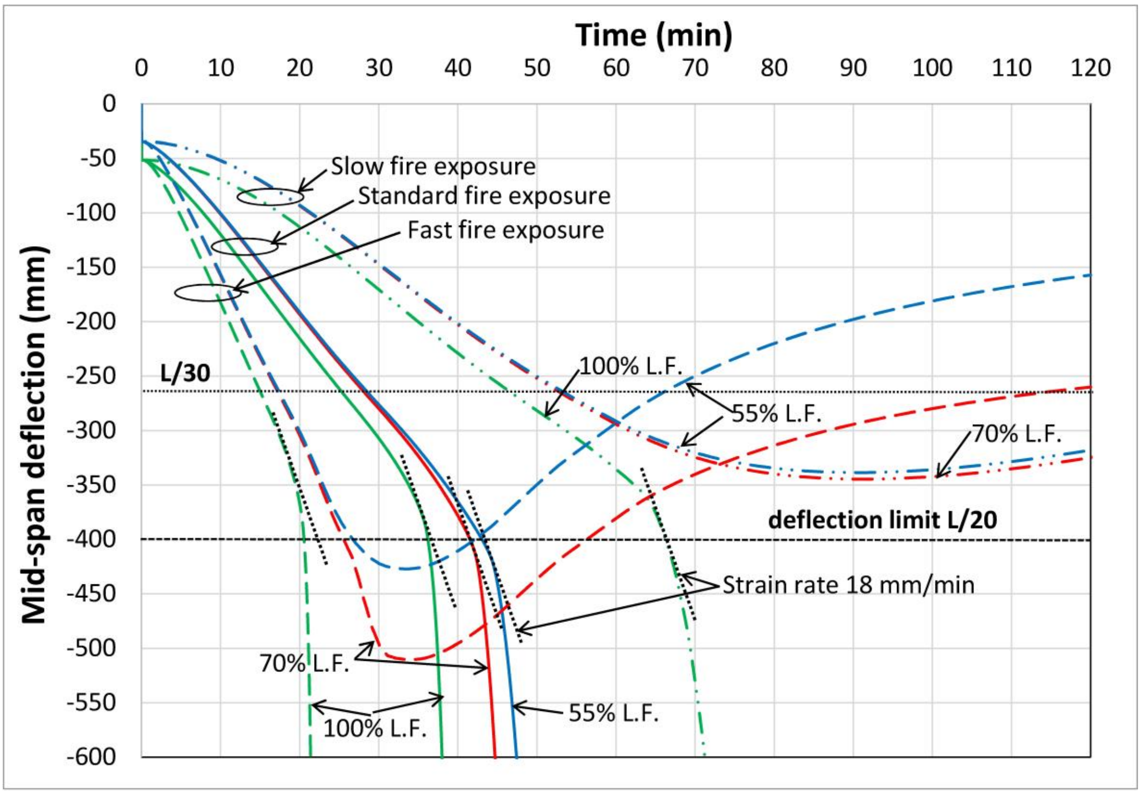

Figure 8. Mid-span deflection vs time for unprotected (a) Beam A and (b) Beam B for 55%, 70% and 100% load factors and different fire exposures (standard, fast, slow).

4.3 Performance of protected USFBs

In this section, the performance of protected USFBs is discussed in terms of developed temperatures (thermal response) and fire resistance (structural response) for three different intumescent coating thicknesses (0.4, 0.8, 1.2 mm).

4.3.1 Thermal response

The temperatures against time relationships are presented in Figure 9. Figure 9 (a) to (c) presents the thermal analysis results for Beam A while Figure 9 (d) to (f) represent Beam B for different fire exposure curves.

Beam A under standard fire exposure develops high average temperatures at the bottom flange (average temperature of node 1 and 2, Figure 9(a)). After 60 minutes of standard fire exposure, the average bottom flange temperatures are 640 ^{o}C, 510 ^{o}C and, 465 ^{o}C for 0.4 mm, 0.8 mm and 1.2 mm thickness of applied intumescent coating, respectively, in comparison with the unprotected beam developed maximum temperature of 775 ^{o}C. After 90 minutes of standard fire exposure, the average bottom flange temperatures are 700 ^{o}C, 605 ^{o}C and, 565 ^{o}C for 0.4 mm, 0.8 mm and 1.2 mm thickness of applied intumescent coating, respectively. After 90 minutes of standard fire exposure the unprotected beam had average bottom flange temperature 895 ^{o}C (Figure 9 (d)). Similarly, Beam B, after 60 min of standard fire exposure had average bottom flange temperature 555 ^{o}C when protected with 0.4 mm of intumescent coating, instead of 740 ^{o}C when unprotected. After 90 minutes of standard fire exposure, the average bottom flange temperature was 630 ^{o}C for 0.4 mm protection, while the unprotected beam developed 860 ^{o}C. The temperatures at nodes 3 and 4 are mostly lower than 400 ^{o}C and so they are not important.

When exposed to fast parametric fire, Beam A at node 1 develops maximum temperature 630 ^{o}C (Figure 9 (b)) when protected with 0.4 mm protection. The average bottom flange temperature is 550 ^{o}C. For 0.8 mm thickness of intumescent coating the maximum average temperature of the bottom flange is 465 ^{o}C. Similarly, Beam B develops maximum average bottom flange temperatures 485 ^{o}C and 360 ^{o}C for 0.4 and 0.8 mm thickness of intumescent coating. Nodes 3 and 4 develop temperatures always lower than 250 ^{o}C and so they do not affect the capacity of the beam.

When Beam A is exposed to slow parametric fire (Figure 9(c)), the maximum developed temperature is 500 ^{o}C and the maximum average temperature of the bottom flange is just 450 ^{o}C when 0.4 mm of intumescent coating is applied. For higher thicknesses of coating, and also at nodes 3 and 4 the temperatures remain low. Similarly, Beam B (Figure 9(f)), under the same conditions develops just 370 ^{o}C maximum average bottom flange temperature for 0.4 mm of protection.

Typical temperature distributions are shown in Tables 4, 5, and 6 for standard, fast and low fire exposure respectively. Furthermore, in these tables, the effect of insulation on the temperature distribution of the cross-section is shown.

(a)

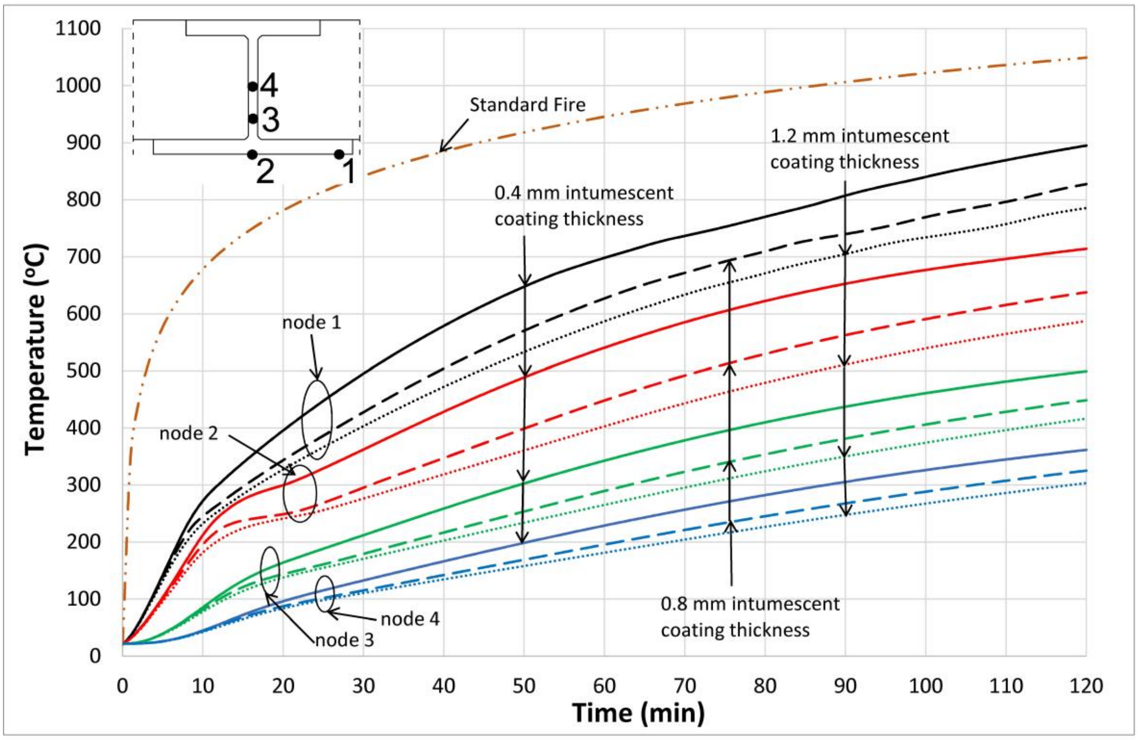
Standard Fire
1.2 mm intumescent coating thickness
0.4 mm intumescent coating thickness
0.8 mm intumescent coating thickness
node 1
node 2
node 3
node 4
4
3
2
1
Temperature (ºC)
Time (min)
0
100
200
300
400
500
600
700
800
900
1000
1100
0
10
20
30
40
50
60
70
80
90
100
110
120

(b)

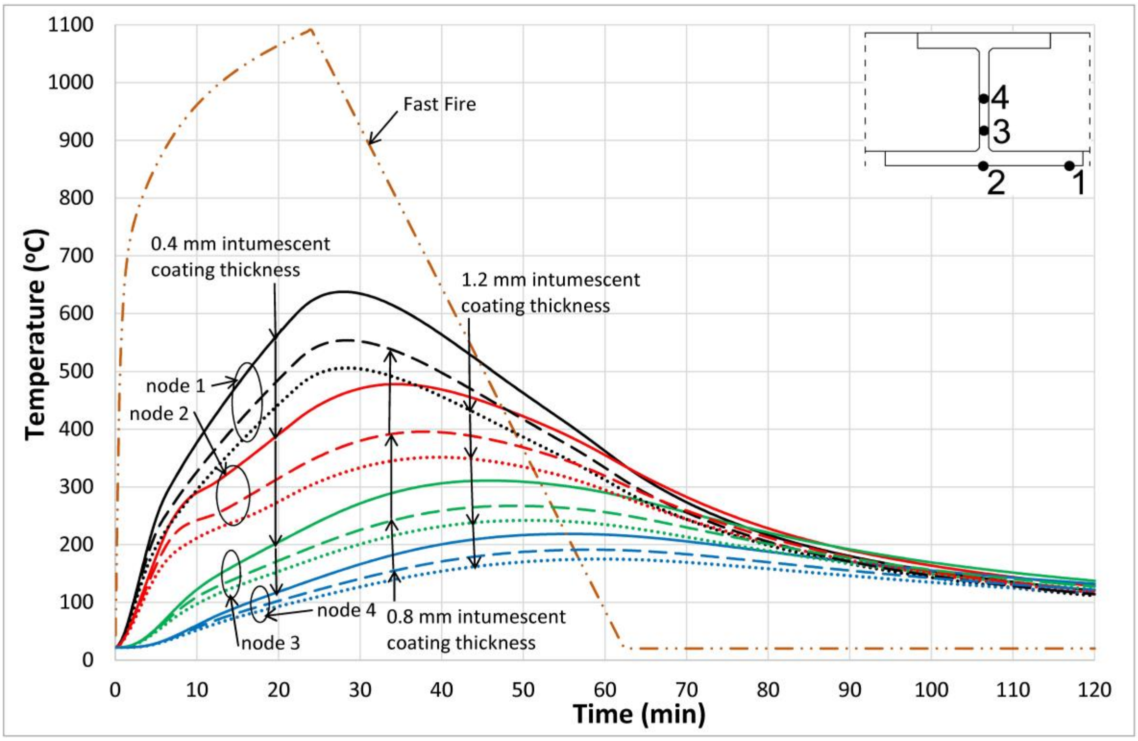
Fast Fire
0.4 mm intumescent coating thickness
1.2 mm intumescent coating thickness
0.8 mm intumescent coating thickness
node 1
node 2
node 3
node 4
4
3
2
1
Temperature (ºC)
Time (min)
0
100
200
300
400
500
600
700
800
900
1000
1100
0
10
20
30
40
50
60
70
80
90
100
110
120

(c)

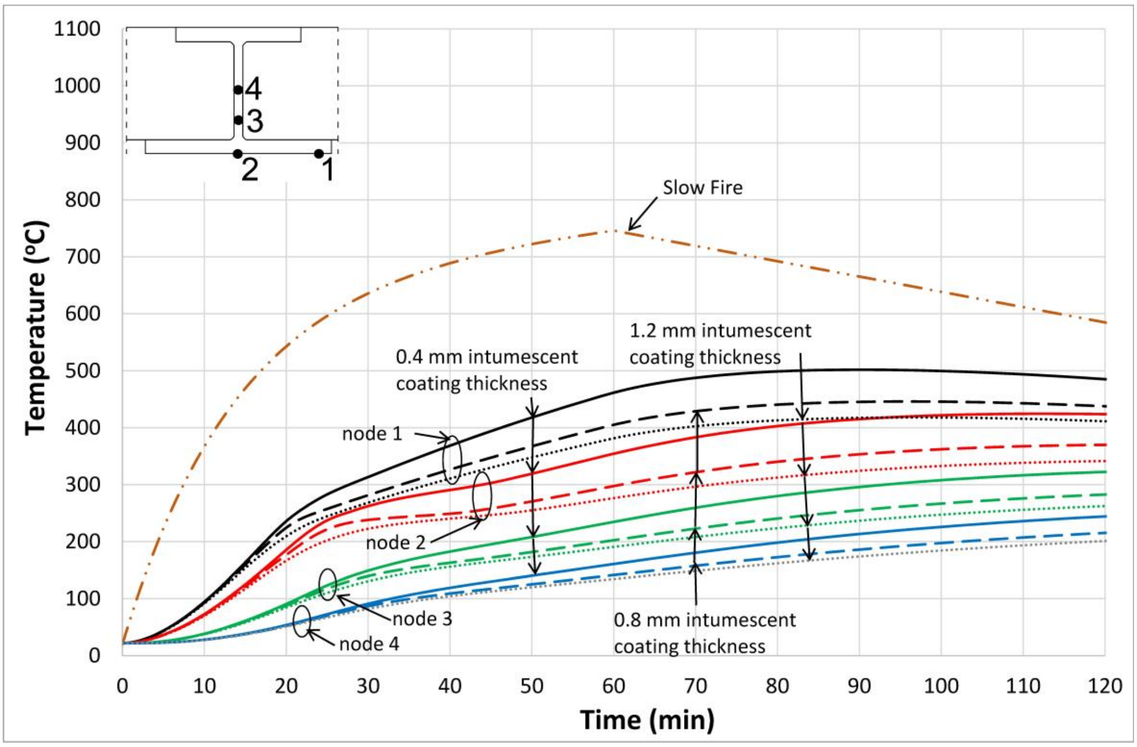
4
3
2
1
Slow Fire
1.2 mm intumescent coating thickness
0.4 mm intumescent coating thickness
node 1
node 2
node 3
node 4
0.8 mm intumescent coating thickness
Temperature (ºC)
Time (min)
1100
1000
900
800
700
600
500
400
300
200
100
0
0
10
20
30
40
50
60
70
80
90
100
110
120

(d)

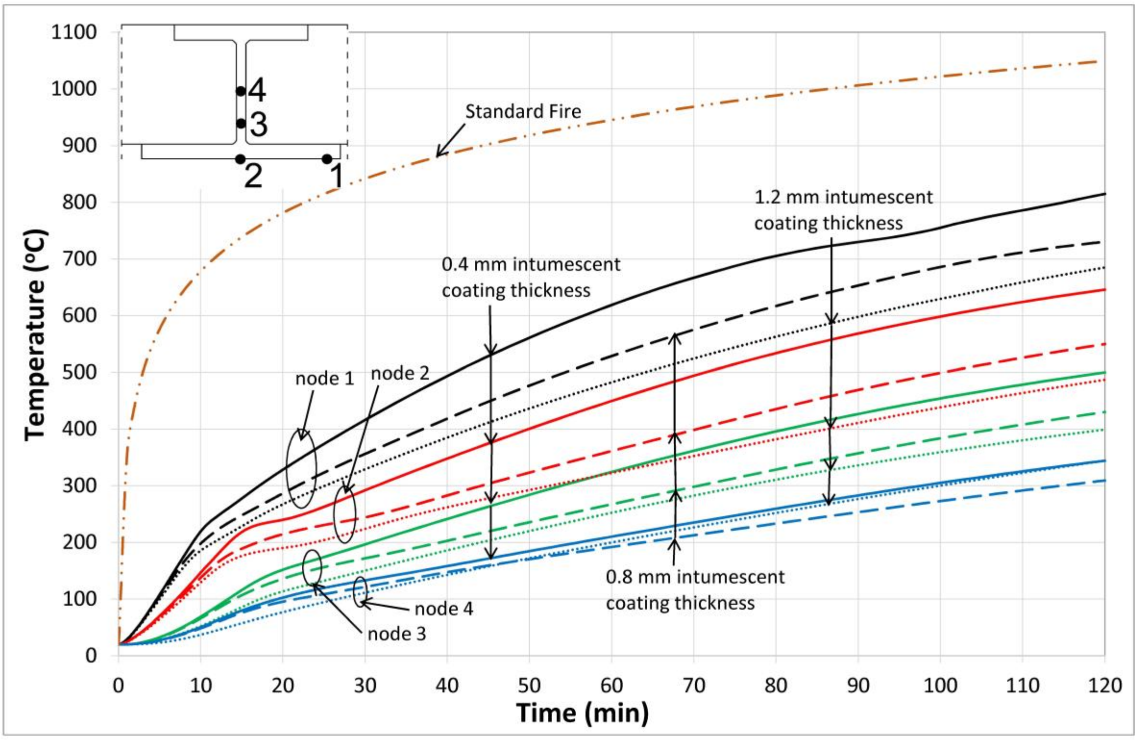
4
3
2
1
Standard Fire
1.2 mm intumescent coating thickness
0.4 mm intumescent coating thickness
node 1
node 2
node 3
node 4
0.8 mm intumescent coating thickness
Temperature (ºC)
Time (min)
1100
1000
900
800
700
600
500
400
300
200
100
0
0
10
20
30
40
50
60
70
80
90
100
110
120

(e)

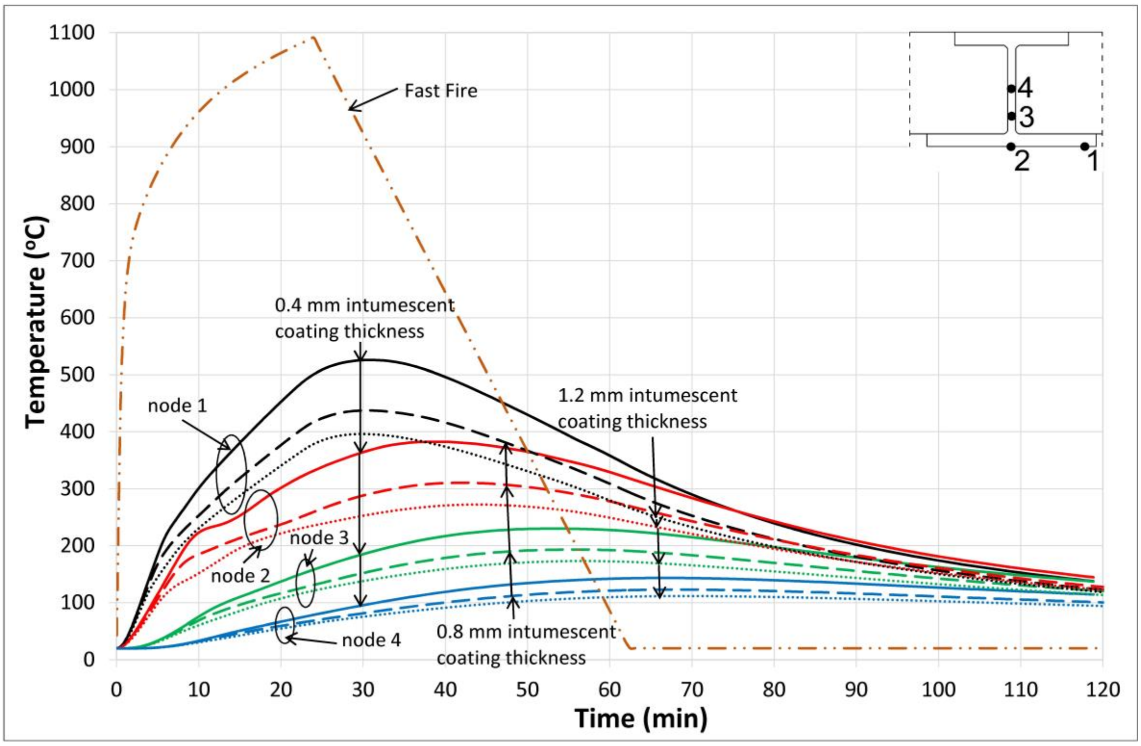

(f)

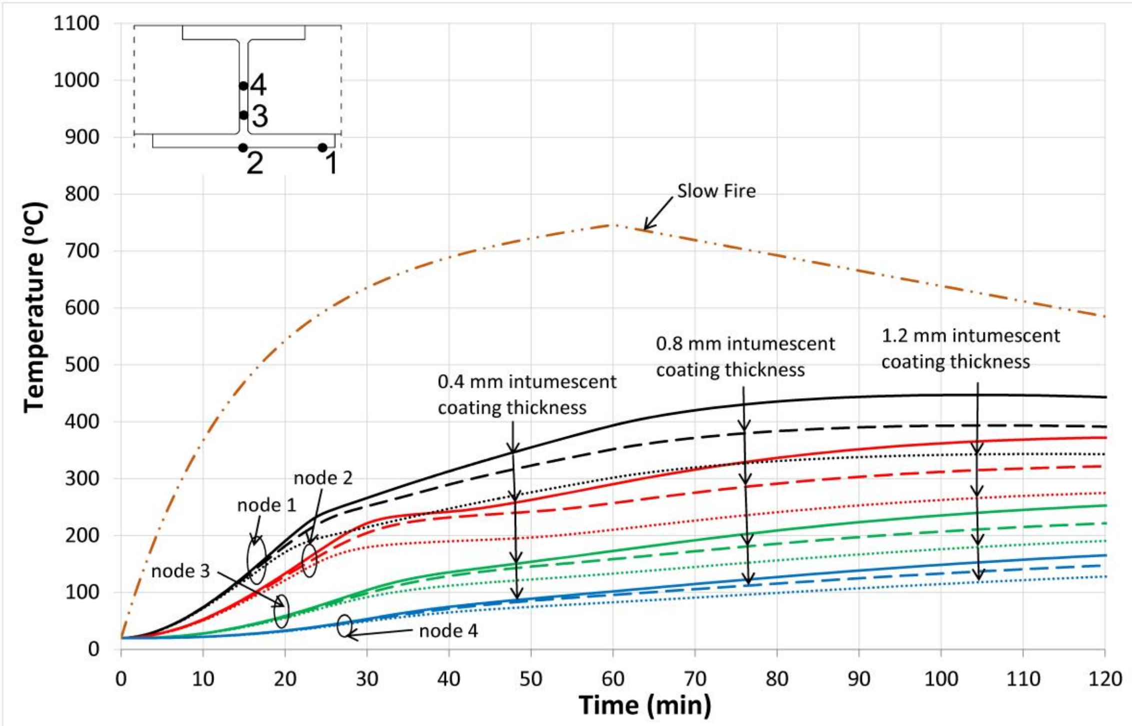

Figure 9. Temperature vs time relationships for Beam A and (a) standard fire, (b) fast fire, (c) slow fire exposure and for Beam B and (d) standard fire, (e) fast fire, (f) slow fire exposure, protected with 0.4, 0.8, and 1.2 mm thickness of intumescent coating.

Table 4 Comparison of temperature development of Beam A after 90 min of standard fire exposure

Node No According Figure 9	temperature (°C) unprotected	Ratio θ_i / θ_1 unprotected	temperature (°C) Protected 0.4 mm	Ratio θ_i / θ_1 Protected 0.4 mm	temperature (°C) Protected 0.8 mm	Ratio θ_i / θ_1 Protected 0.8 mm	temperature (°C) Protected 1.2 mm	Ratio θ_i / θ_1 Protected 1.2 mm
1	967.46	1	808.14	1	739.85	1	705.56	1
2	898.71	0.929	653.07	0.81	562.76	0.76	511.60	0.72
3	570.50	0.59	437.85	0.54	381.45	0.52	350.78	0.50
4	387.93	0.40	305.67	0.38	267.79	0.36	248.02	0.35

Table 5 Temperature development in Beam A when temperature is maximum at node 1 for fast fire exposure

Node No According Figure 9	temperature (°C) unprotected t=25.91 min	Ratio θ_i / θ_1 unprotected	temperature (°C) Protected 0.4 mm t=27.95 min	Ratio θ_i / θ_1 Protected 0.4 mm	temperature (°C) Protected 0.8 mm t=28.41 min	Ratio θ_i / θ_1 Protected 0.8 mm	temperature (°C) Protected 1.2 mm t=28.24 min	Ratio θ_i / θ_1 Protected 1.2 mm
1	795.82	1	637.60	1	553.48	1	505.55	1
2	680.44	0.86	461.19	0.72	372.65	0.67	325.60	0.64
3	338.34	0.43	259.58	0.41	217.81	0.39	193.08	0.38
4	189.03	0.24	156.69	0.25	135.03	0.24	121.06	0.24

Table 6 Temperature development in Beam A when temperature is maximum at node 1 for slow fire exposure

Node No According Figure 9	temperature (°C) unprotected t=71.06 min	Ratio θ_i / θ_1 unprotected	temperature (°C) Protected 0.4 mm t=91.11 min	Ratio θ_i / θ_1 Protected 0.4 mm	temperature (°C) Protected 0.8 mm t=96.39 min	Ratio θ_i / θ_1 Protected 0.8 mm	temperature (°C) Protected 1.2 mm t=97.06 min	Ratio θ_i / θ_1 Protected 1.2 mm
1	650.88	1	501.86	1	446.06	1	418.19	1
2	576.05	0.89	416.22	0.83	359.47	0.80	330.77	0.79

3	369.59	0.57	297.46	0.59	262.94	0.59	244.47	0.58
4	246.59	0.38	214.88	0.42	193.60	0.43	181.50	0.43

4.3.2 Structural Response

The structural response of beams A and B for different fire conditions and load factors in terms of fire resistance as defined in BS476-Part 20 (1987) [19] is presented in Figure 10.

Both beams survive the parametric fires even when protected with the minimum of 0.4 mm of intumescent coating, for all examined load factors. During cooling phase, the bottom flange temperatures are reduced, so the bowing effect is reduced and gradually the beam is returning to its initial shape, eg the deflection due to temperature is disappearing.

The fire resistance of both beams under standard fire exposure is presented in Table 7.

(a)

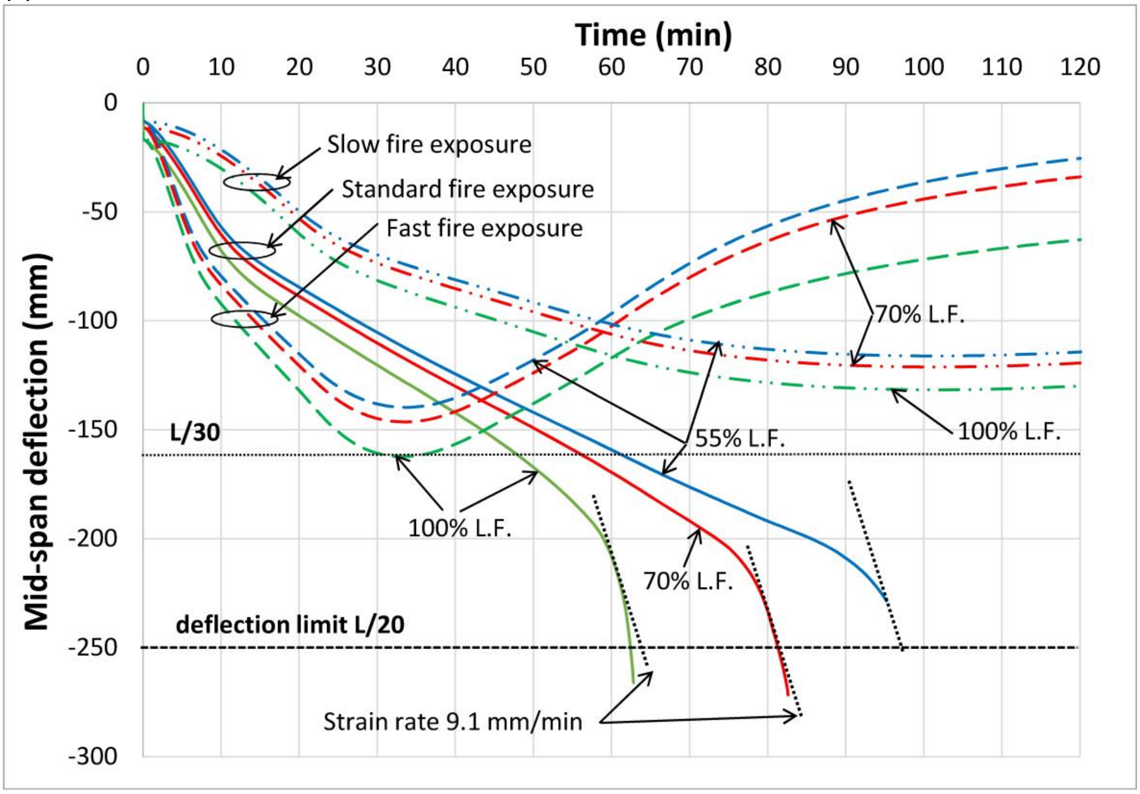

(b)

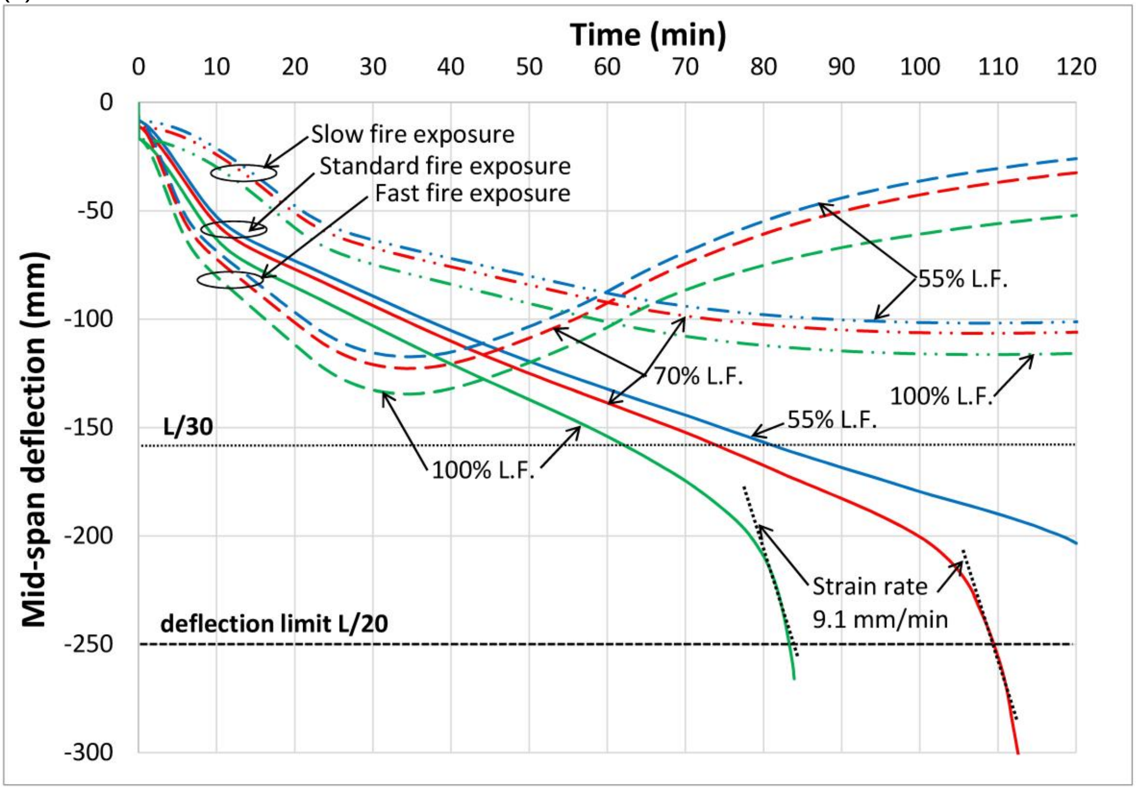
Time (min)
0
10
20
30
40
50
60
70
80
90
100
110
120
Mid-span deflection (mm)
0
-50
-100
-150
-200
-250
-300
Slow fire exposure
Standard fire exposure
Fast fire exposure
55% L.F.
70% L.F.
100% L.F.
100% L.F.
55% L.F.
L/30
Strain rate
9.1 mm/min
deflection limit L/20

(c)

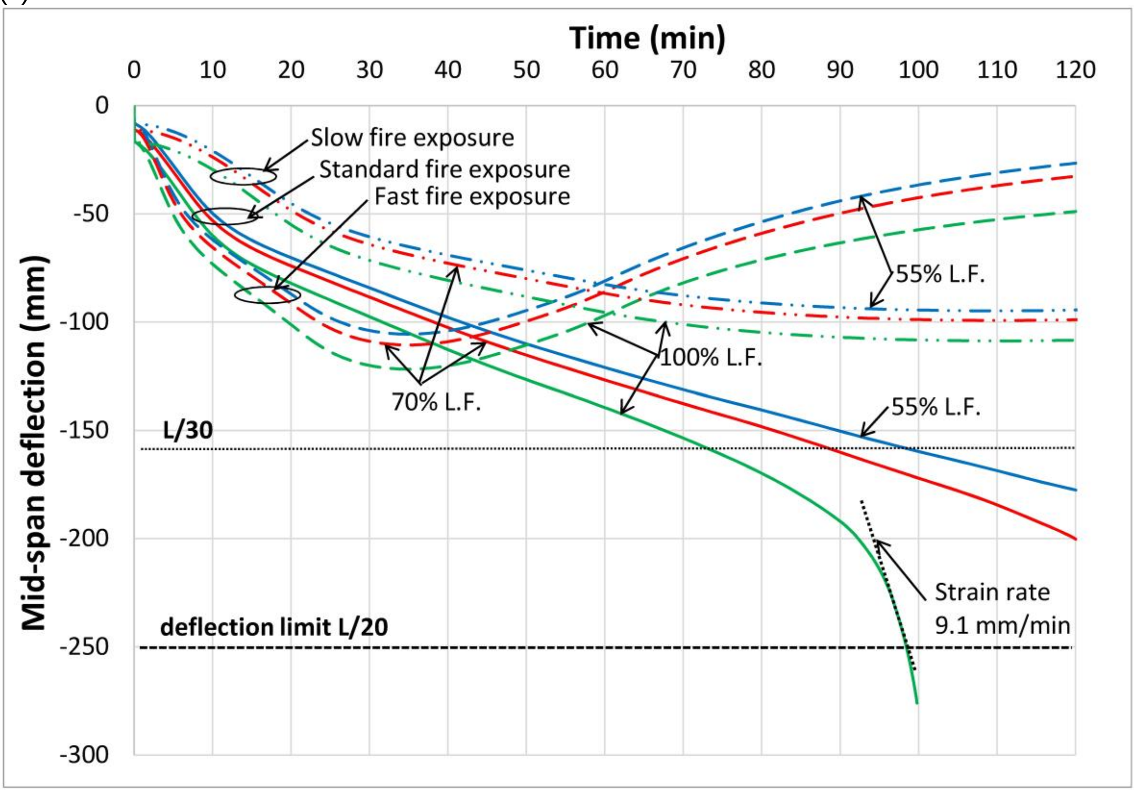
Time (min)
0
10
20
30
40
50
60
70
80
90
100
110
120
Mid-span deflection (mm)
0
-50
-100
-150
-200
-250
-300
Slow fire exposure
Standard fire exposure
Fast fire exposure
55% L.F.
100% L.F.
70% L.F.
55% L.F.
L/30
Strain rate
9.1 mm/min
deflection limit L/20

(d)

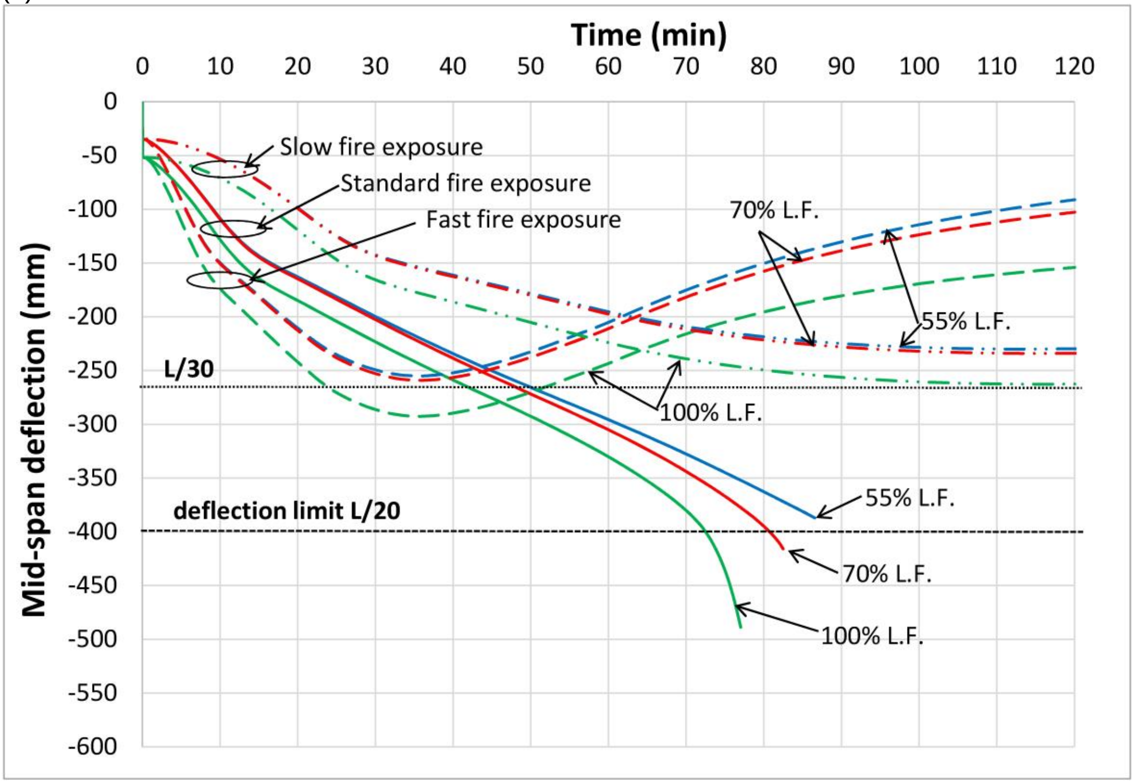
Time (min)
0
10
20
30
40
50
60
70
80
90
100
110
120
Mid-span deflection (mm)
0
-50
-100
-150
-200
-250
-300
-350
-400
-450
-500
-550
-600
Slow fire exposure
Standard fire exposure
Fast fire exposure
70% L.F.
55% L.F.
L/30
100% L.F.
55% L.F.
deflection limit L/20
70% L.F.
100% L.F.

(e)

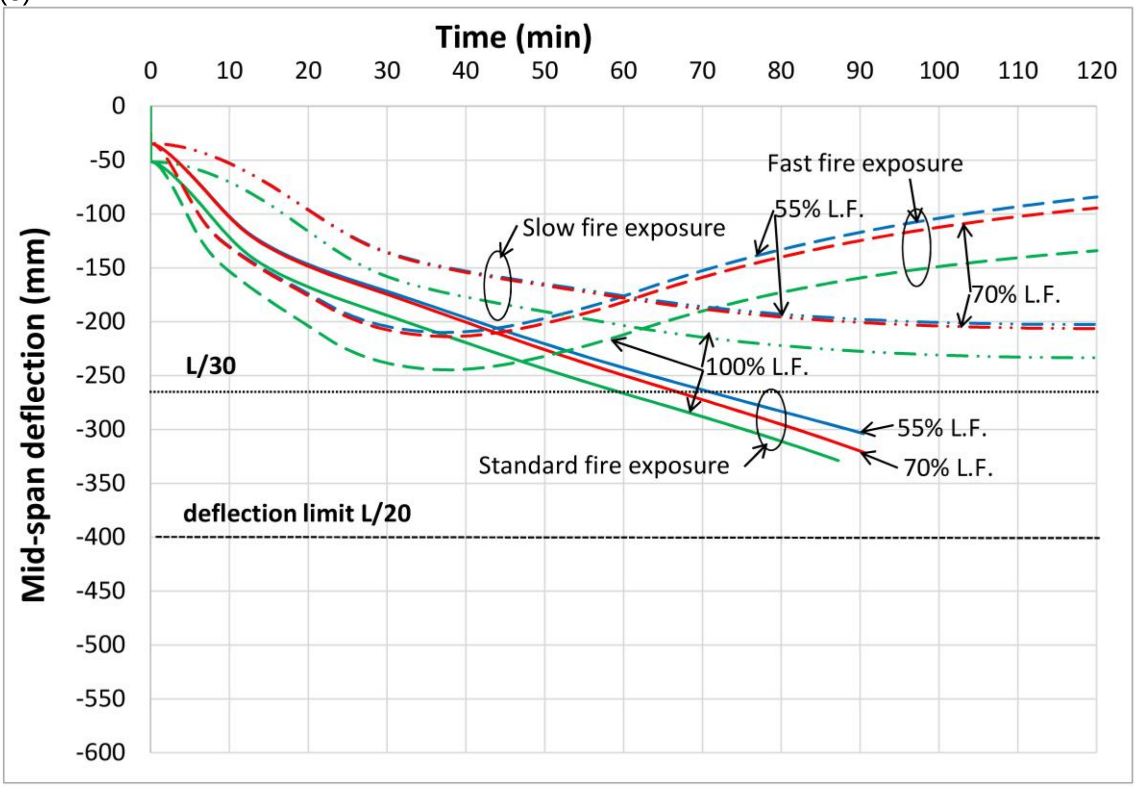
Time (min)
0
10
20
30
40
50
60
70
80
90
100
110
120
Mid-span deflection (mm)
0
-50
-100
-150
-200
-250
-300
-350
-400
-450
-500
-550
-600
Fast fire exposure
55% L.F.
Slow fire exposure
70% L.F.
L/30
100% L.F.
55% L.F.
Standard fire exposure
70% L.F.
deflection limit L/20

(f)

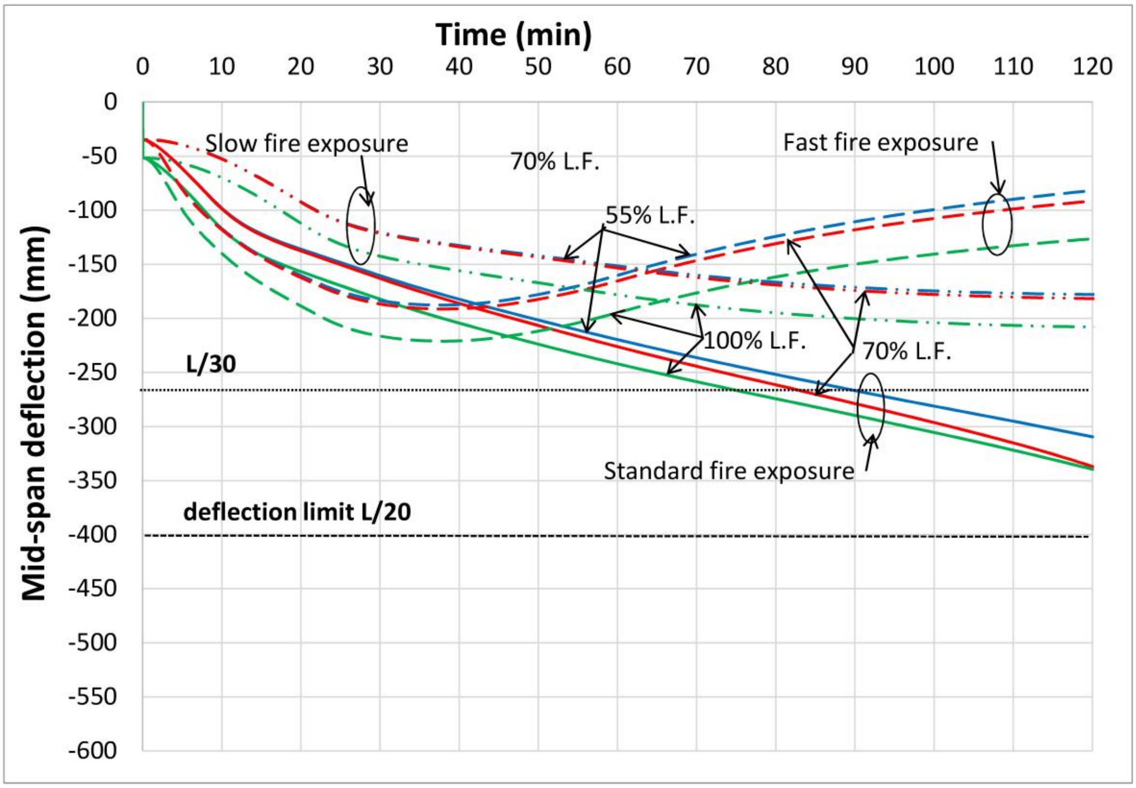

Figure 10. Mid-span deflection vs time for Beam A protected with (a) 0.4 mm, (b) 0.8 mm, (c) 1.2 mm thickness of intumescent coating and Beam B protected with (d) 0.4 mm, (e) 0.8 mm, (f) 1.2 mm thickness of intumescent coating for 55%, 70% and 100% load factors and different fire exposures (standard, fast, slow).

Table 7. Fire resistance of protected beams A and B under standard fire exposure for different intumescent coating thicknesses and different load factors.

	Fire Resistance (min)					
	Beam A			Beam B		
	Load factor			Load factor		
Thickness of intumescent coating (mm)	100%	70%	55%	100%	70%	55%
0.4	60	80	90	60	70	80
0.8	80	100	120	80	90	100
1.2	90	120	120	120	120	120

5. Discussion

The critical temperature according EN 1994-1-2 (2005), for beam A is 385 ^{o}C and for beam B 460 ^{o}C as calculated in Maraveas et al (2015)[6], defined as average bottom flange temperature. As it is seen in Figures 7-10, these critical temperatures are very conservative. For example, unprotected beam A survives the slow fire, with average bottom flange temperature 575 ^{o}C even for the non-realistic load factor of 100% (Figure 7(c) and Figure 8(a)). The same unprotected beam fails after approximately 35 min exposure to the standard fire and when the average bottom flange temperature is approximately 600 ^{o}C (Figure 7(a) and Figure 8(a)). The difference, in terms of critical temperatures, between EN 1994-1-2 (2005) [7] and the FEM results is relevant to the stress redistribution when the bottom flange is very hot and the contribution of the concrete slab. Most flooring systems with partially protected cross-section in fire experience similar performance [21]. The bottom flange temperatures are function of the cross-section factor, eg of the exposed flange section factor. Thicker flanges will develop lower temperatures and will have improved performance in fire. Similarly, the thickness of the steel web also has a role in fire resistance of the USFBs. A USFB with thicker web, especially the bottom half, give a better fire resistance. Further, the depth of the USFBs may dictate their fire resistance as the thermal gradient plays a vital role in their fire performance. For deeper USFBs, the thermal gradient may be higher and for shallower USFBs, the thermal gradient may be lower. For similar thicknesses of the flanges and steel web, a USFB with larger depth may provide a higher fire resistance as compared to a USFB with a smaller overall depth.

When the beams are exposed to parametric fires, they survive with just a minimum of protection. This leads to low cost solution, compatible with the predictions of Eurocodes and in parametric fire exposures. Parametric fires are realistic, on the contrary, the standard fire is non-realistic and it is used for historical reasons.

This research is limited to simply supported beams. More complex structural systems need further research and the conclusions of this research may not applied.

6. Concluding remarks

The paper presents a numerical investigation on the performance of Ultra Shallow Floor Beams exposed to standard and parametric fires. Two different simply supported USFBs with different span lengths and cross-sections have been examined under different fire exposure conditions and load factors. Both unprotected and protected beams were considered with intumescent coating of three different thicknesses. From the FEM results, the following conclusions can be drawn:

- Although it is a common practice to apply the fire protection materials on the bottom exposed steel flange of the USFBs, it was found that USFBs can survive slow parametric fires under realistic load factors without the fire protection materials. This will help with reducing the cost of structures without comprising their fire resistance. The reduction in the application of fire protection materials should always be based on the results of performance-based design. For example, during this study, it was found that with a layer of 0.4 mm intumescent coating the USFBs can survive a full duration of a compartment (fast or slow) fire.
- Like other structural members, the increase in thickness of the fire protection material helps in achieving a higher fire resistance of USFBs. During this study, the minimum thickness of the applied intumescent coating as fire protection material was 0.4 mm. It was found that the USFBs can survive both fast and slow parametric fire exposures under any realistic load factor when protected with 0.4 mm thickness of intumescent coating. This thickness of the applied fire protection material is significantly lesser than the current practice used during construction. Further research is required for cross-sections with different section factors.
- It was found that the fire resistance of USFBs is sensitive to the applied load factor as well as to the type of fire exposure irrespective of the level of the applied fire protection. USFBs with a lesser thickness of the fire protection materials underwent larger deflections as compared to the USFBS with higher thickness of the fire protection under similar applied loads.
- Although the USFBs offer a good fire resistance with little or no fire protection when exposed to fast and slow parametric fires respectively, their response in standard fires is more demanding. USFBs can only reach high levels of fire resistance (like R90 and R120) when exposed to standard fires only with the aid of a thick intumescent coating or combination of intumescent coating and low load ratio.
- The fire design approach proposed for composite beams in EN1994-1-2 (2005) is more suitable for steel-concrete beams with hanging steel beam sections. These design approaches when applied to USFBs produce safe but highly conservative and uneconomical results. The outcomes of this study have shown that the current fire

design recommendations given in EN1994-1-2 (2005) needs to be modified. There is a need to develop similar fire design approaches which are less conservative and more suited to USFBs.

Acknowledgements

The authors would like to thank Professor Yong C. Wang, School of Mechanical, Aerospace and Civil Engineering, University of Manchester, for his guidance relate to the thermal conductivity and other properties of intumescent coatings.

References

1. Ahmed, I.M., Tsavdaridis K.D. (2019), The evolution of composite flooring systems: applications, testing, modelling and eurocode design approaches, Constructional Steel Research, 155, pp 286-300.
2. Tsavdaridis, K.D., D'Mello, C. and Huo, B.Y. (2009). Computational study modelling the experimental work conducted on the shear capacity of perforated concrete-steel Ultra Shallow Floor Beams (USFB). In Proceedings of 16th Hellenic Concrete Conference (p. 159).
3. Huo B. Y. and D'Mello C. A. (2013), Push-out tests and analytical study of shear transfer mechanisms in composite shallow cellular floor beams, Constr. Steel Res., vol. 88, pp. 191–205.
4. Tsavdaridis K. D., D'Mello C., and Huo B. Y. (2013), "Experimental and computational study of the vertical shear behaviour of partially encased perforated steel beams," Eng. Struct., vol. 56, no. January, pp. 805–822.
5. Kansinally, R. and Tsavdaridis, K.D. Vibration Response of USFB Composite Floors. The 13th Nordic Steel Construction Conference (NSCC 2015). 23-25 September, 2015, Tampere, Finland.
6. Maraveas C., Tsavdaridis K. D. and Nadjai A. (2015), Fire resistance of unprotected Ultra Shallow Floor Beams (USFB) A numerical investigation, Fire Technol., 53, pp 609-627.
7. EN 1994-1–2: (2014). Eurocode 4, part 1-2: Design of composite steel and concrete structures - General rules — Structural fire design. European Committee for Standardization.
8. Alam, N., Nadjai, A., Maraveas, C., Tsavdaridis, K.D. and Ali, F. (2018) Response of Asymmetric Slim Floor Beams in Parametric Fires. Journal of Physics: Conference Series, 1107, 032009
9. Maraveas, C., Wang, Y.C., Swailes, T. (2017), Reliability based determination of material safety factor for cast iron beams in jack arched construction exposed to standard and natural fires, Fire Safety Journal, 90, pp 44-53.

10. Maraveas, C., Swailes, T. & Wang, Y., (2012). A detailed methodology for the finite element analysis of asymmetric slim floor beams in fire. Steel Construction, 5 (3), pp 191-198.
11. Tsavdaridis, K.D., D'Mello, C. and Hawes, M. Experimental Study of Ultra Shallow Floor Beams (USFB) with Perforated Steel Sections. The 11th Nordic Steel Construction Conference 2009 (NSCC 2009). 2-4 September 2009, Malmö, Sweden, Reference no: 128, pp. 312-319.
12. de Silva D., Bilotta A., Nigro E. (2019). Experimental investigation on steel elements protected with intumescent coating. Constr Build Mater, 205, pp. 232-244
13. Cirpici B.K., Wang Y.C., Rogers B. (2016). Assessment of the thermal conductivity of intumescent coatings in fire. Fire Safety Journal. 81, pp 74-84
14. Dai X., Wang Y.C. and Bailey C. (2010). A Simple Method to Predict Temperatures in Steel Joints with Partial Intumescent Coating Fire Protection. Fire Technology, 46. pp 19–35
15. EN1991-1-2 (2009), Eurocode 1 – Actions on structures – Part 1–2: General Rules – Structural Fire Design, European Committee for Standardization.
16. Alam, N., Nadjai, A., Ali, F., & Nadjai, W. (2018). Structural response of unprotected and protected slim floors in fire. Constructional Steel Research, 142, pp.44–54.
17. Bourbigot S., Le Bras M., Delobel R. (1995). Fire Degradation of an Intumescent Flame Retardant Polypropylene using the Cone Calorimeter. Journal of Fire Sciences. https://doi.org/10.1177/073490419501300101
18. Bailey, C.G., (1999). The behaviour of asymmetric slim floor steel beams in fire. Journal of Constructional Steel Research, 50(3), pp.235–257.
19. BS 476 Part-20 (1987). Fire tests on building materials and structures. Method for determination of the fire resistance of elements of construction
20. ISO 834–1 (1999) Fire-resistance tests—elements of building construction—part 1: general requirements. ISO, Switzerland.
21. SCI (2008) Steel Construction Institute, Slimflor compendium, Document RT1147